7

Grey-body radio-emission

The purpose of this chapter is to consider the basic characteristics of the radiation field of one of the most important and widely used physical models of natural objects, namely, the grey half-space with a smooth boundary. Definitions of the reflective and polarization properties of such media are introduced. The physical features of polarized radiation reception by microwave complexes are analysed. Using the impedance forms of boundary conditions of the Maxwellian equations, the model for calculating the plane-parallel layered media is formulated. This model is widely used in the theory and practice of passive microwave remote sensing. On the basis of the plane-parallel layered media method the electrodynamic problem of radio-emission of inhomogeneous non-isothermal media is analysed in detail. The results and limitations of the quasi-monochromatic approach to calculating the radiation characteristics of layered media are considered, in particular, the quasi-coherency properties of a noise signal with a limited spectrum as applied to the problem of emission of a two-layered medium.

7.1 SURFACE REFLECTIVITY

Before proceeding to the basic subject of this chapter, we note that by grey physical bodies we shall mean physical objects whose radiation properties differ from the radiation of ideal black bodies in the wavelength band under consideration. Or, in other words, physical objects, whose emissivity differs from unity (and whose wavelength (frequency) dependence can be rather intricate, generally speaking), can serve as a source of quite valuable remote information. The physical reasons for this can be quite diverse: the physical-chemical properties of a medium, the degree of a surface roughness, the temperature properties, the subsurface structures (inhomogeneities) and others. Note that in the other wavelength bands (for example, in the IR band) by the 'grey' term are meant, generally speaking, the other features of

radiation, for example, the independence of the spectral emissivity from the wavelength (Siegel and Howell, 1972).

It is much more complicated to determine the reflective properties of a surface element than the emissivity or absorbing ability (see section 6.3). This is explained by the fact that the reflectivity of a surface depends not only on its physical properties and on the physical body's temperature, but also on the directions of incident and reflected radiation. In general, the study of the reflective properties of surfaces is a very complex problem. Various definitions and approaches are used in the science and science-technological literature for the description and investigation of radiation reflection from a surface element. In the physics literature the whole of the class of these definitions is sometimes defined as scattering indicatrix (Prochorov, 1984). The discussion of various concepts accepted in optics and radiophysics can be found in books by Peake (1959); Siegel and Howell (1972); Ozisik (1973); Skolnik (1980); Ishimaru (1978, 1991). We have no scope to analyse in detail these concepts and the relationships between them within the framework of this book. Here we shall consider only those concepts that concern radiation reflection from surfaces and that we will need later.

7.1.1 Reflection distribution function

Consider a monochromatic radiation beam of intensity $I_\nu(\mathbf{r}, \mathbf{\Omega}')\,\mathrm{d}\Omega'$, which falls on the surface element $\mathrm{d}A$. Let θ' be the angle between the incident beam and the normal to the surface (Figure 7.1). The quantity of energy of radiation, falling on a unit area of the surface element per unit of time in a unit range of frequencies, is equal to

$$I_\nu(\mathbf{r}, \mathbf{\Omega}')\cos\theta'\,\mathrm{d}\Omega'. \tag{7.1}$$

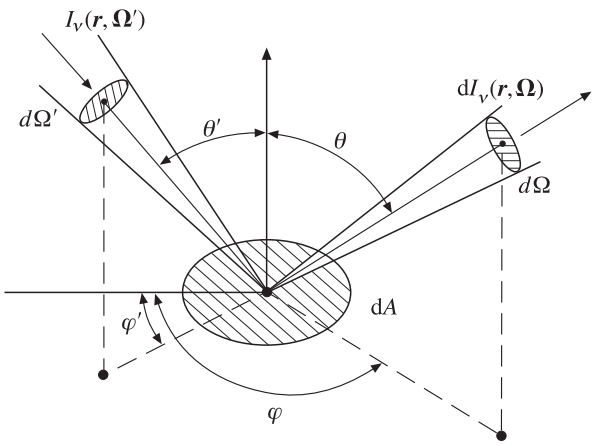

Figure 7.1. Schematic beam representation of the incident and reflected radiations for the determination of bidirectional reflectivity.

Some part of this radiation will be reflected by the surface in all directions within the limits of a hemispherical solid angle. Let $\mathrm{d}I_\nu(\mathbf{r}, \mathbf{\Omega}')$ be the intensity of radiation reflected in the direction of observation $\mathbf{\Omega}$. The reflected radiation intensity is related to the incident radiation energy by the spectral distribution function (or by the bidirectional reflectivity) of the reflected radiation (the reflection indicatrix) $f_\nu(\mathbf{r}, \mathbf{\Omega}', \mathbf{\Omega})$ defined as follows:

$$f_\nu(r, \mathbf{\Omega}', \mathbf{\Omega}) = \frac{\mathrm{d}I_\nu(\mathbf{r}, \mathbf{\Omega})}{I_\nu(\mathbf{r}, \mathbf{\Omega}') \cos\theta' \, \mathrm{d}\Omega'}. \tag{7.2}$$

The quantity so defined can be either greater or less than unity, depending on the surface structure. For example, for mirror-reflecting surfaces the total incident radiation comprised within the limits of solid angle $\mathrm{d}\Omega'$, is reflected within the limits of solid angle $\mathrm{d}\Omega = \mathrm{d}\Omega'$, whose axis is the direction determined by angles $\theta = \theta'$ and $\varphi = \varphi' \pm \pi$.

Using the generalized reciprocity theorem, which was first formulated by Helmholtz, it can be shown (Siegel and Howell, 1972), that the reflection indicatrix is symmetric with respect to incidence and reflection directions:

$$f_\nu(\mathbf{r}, \mathbf{\Omega}', \mathbf{\Omega}) = f_\nu(\mathbf{r}, \mathbf{\Omega}, \mathbf{\Omega}'). \tag{7.3}$$

The reflective properties of the surface are completely defined, if the reflection indicatrix is known for all directions of a hemispherical space. However, it is extremely difficult to obtain such information experimentally; for this reason the total reflection indicatrix is not used, as a rule, in remote sensing practice. The integral (averaged over angles) reflective characteristics are widely used in IR sensing practice. In its turn, the integrally angular approach is seldom applied in microwave sensing.

7.1.2 Directional-hemispherical reflectivity

In the case where the surface is rather rough with respect to the electromagnetic field wavelength, the situation can arise in which the surface is irradiated by the radiation beam from a given direction, and the reflected radiation is scattered within the limits of a hemispherical solid angle (over the surface). A similar scattering regime is characteristic of terrestrial surfaces when they are irradiated by sunlight as well as by IR radiation sources. In this case the spectral directional-hemispherical reflectivity $\rho_\nu(\mathbf{r}, \mathbf{\Omega}' \to 2\pi)$ is determined as follows:

$$\rho_\nu(\mathbf{r}, \mathbf{\Omega}' \to 2\pi) = \frac{\int_{\Omega=2\pi} \mathrm{d}I_\nu(\mathbf{r}, \mathbf{\Omega}) \cos\theta \, \mathrm{d}\Omega}{I_\nu(\mathbf{r}, \mathbf{\Omega}') \cos\theta \, \mathrm{d}\Omega'}. \tag{7.4}$$

Using the definition of the reflection indicatrix, we can relate $\rho_\nu(\mathbf{r}, \mathbf{\Omega}' \to 2\pi)$ with $f_\nu(\mathbf{r}, \mathbf{\Omega}', \mathbf{\Omega})$ as follows:

$$\rho_\nu(\mathbf{r}, \mathbf{\Omega}' \to 2\pi) = \int_{\varphi=0}^{2\pi} \int_{\mu=0}^{1} f_\nu(r; \mu', \varphi'; \mu, \varphi) \mu \, \mathrm{d}\mu \, \mathrm{d}\varphi. \tag{7.5}$$

The case is often considered, which is opposite to that described above, when the radiation falls on the surface element from all directions within the limits of a hemispherical solid angle (over the surface), and the reflected radiation intensity is measured only in the given direction $\mathbf{\Omega}$. In such a case the hemispherically directional reflectivity $\rho_\nu(\mathbf{r}, 2\pi \to \mathbf{\Omega})$ can be presented (provided that the incident radiation does not depend on the direction) in the form:

$$\rho_\nu(r, 2\pi \to \mathbf{\Omega}) = \int_{\varphi'=0}^{2\pi} \int_{\mu'=0}^{1} f_\nu(\mathbf{r}; \mu', \varphi'; \mu, \varphi) \mu' \, \mathrm{d}\mu' \, \mathrm{d}\varphi'. \tag{7.6}$$

Using the reciprocity theorem, it can easily be seen that in the case where $\varphi = \varphi'$ and $\theta = \theta'$, the following equality is met:

$$\rho_\nu(\mathbf{r}, \mathbf{\Omega}' \to 2\pi) = \rho_\nu(\mathbf{r}, 2\pi \to \mathbf{\Omega}). \tag{7.7}$$

7.1.3 Hemispherical reflectivity

Consider the situation where radiation falls on a surface from all directions within the limits of a hemisphere (above the surface) and is reflected in all directions as well. This situation is typical of the case where terrestrial surfaces are irradiated by solar radiation scattered by dense cloudiness (diffuse illumination). With allowance for the definition of a directional-hemispherical reflectivity (7.4) the spectral hemispherical reflectivity $\rho_\nu(\mathbf{r})$ is determined as follows:

$$\rho_\nu(\mathbf{r}) = \frac{\iint_{\Omega'=2\pi} \rho_\nu(\mathbf{r}, \mathbf{\Omega}' \to 2\pi) I_\nu(\mathbf{r}, \mathbf{\Omega}') \cos\theta' \, \mathrm{d}\Omega'}{\iint_{\Omega'=2\pi} I_\nu(\mathbf{r}, \mathbf{\Omega}') \cos\theta' \, \mathrm{d}\Omega'}. \tag{7.8}$$

If the incident radiation does not depend on the direction, then, with allowance for (7.5), we obtain the relation between the reflection indicatrix and $\rho_\nu(\mathbf{r})$

$$\rho_\nu(\mathbf{r}) = \frac{1}{\pi} \int_{\mathbf{\Omega}'=2\pi} \left[\int_{\mathbf{\Omega}=2\pi} f_\nu(\mathbf{r}, \mathbf{\Omega}', \mathbf{\Omega}) \cos\theta \, \mathrm{d}\Omega \right] \cos\theta' \, \mathrm{d}\Omega'. \tag{7.9}$$

If $f_\nu(\mathbf{r}, \mathbf{\Omega}', \mathbf{\Omega})$ does not depend on directions (or, in other words, has diffuse character of scattering), expression (7.9) is simplified and takes the form:

$$\rho_\nu(\mathbf{r}) = \pi f_\nu(\mathbf{r}). \tag{7.10}$$

7.1.4 Diffuse and specular reflection

The surface is called a diffuse reflector if the intensity of reflected radiation is the same over all angles of reflection within the limits of a hemisphere and does not depend on the angle of incidence. The surface is called a specular or mirror reflector if the incident and reflected beams are symmetrical with respect to the normal at the point of incidence, and the reflected beam is concluded inside the solid angle $\mathrm{d}\Omega$ equal to a solid angle containing the incident beam $\mathrm{d}\Omega'$ (i.e. $\mathrm{d}\Omega = \mathrm{d}\Omega'$). The

assumption on diffuse and specular reflections is often used in the theory and practice of remote sensing, of heat transfer, since it results in considerable simplifications; the real surfaces, however, are neither ideally diffuse, nor ideally specular. We should note here, that, depending on the wavelength used and on the degree of surface roughness, the contributions of specular and diffuse components in the process of full scattering by a studied medium can drastically differ. So, in the optical and IR bands the majority of solid terrestrial media (including vegetation) represent diffuse reflectors. At the same time, the disturbed sea surface represents the most complicated (and dynamical) combination of diffuse and quasi-specular reflectors (the field of patches of sunlight) (Figure 2.1). In the microwave band the specular component plays a noticeable part, both for electromagnetic waves scattering on the sea surface and for scattering on the land surface. In its turn, the vegetation can be presented, depending on the wavelength, either as a highly diffuse (scattering) object, or as an ideal black body (an ideal absorber), or as their complicated scattering–absorbing combination of fractal type (see, for example, Peake, 1959; Fung and Chen, 1981; Franceschetti *et al.*, 1999a,b; Chauhan, 2002; Wu and Liu, 2002; Miesch *et al.*, 2002). Generally speaking, it is the choice of the most adequate scattering model of a studied surface which represents, to a considerable degree, the modern problem of microwave radiation of rough terrestrial covers (such as the disturbed sea surface, vegetation, the processed surface of soils and grounds) (see Chapter 12 for more details).

7.2 EFFECTIVE RADIATION OF REFLECTING SURFACE

Let us consider a beam of monochromatic radiation of intensity $I_\nu(\mathbf{r}, \mathbf{\Omega}')\,\mathrm{d}\Omega'$, which falls on the surface element $\mathrm{d}A$ (Figure 7.1). The quantity of the energy of radiation, falling on the surface area unit per unit time, within a unit frequency band, is equal to $I_\nu(\mathbf{r}, \mathbf{\Omega}')\cos\theta'\,\mathrm{d}\Omega'$, where θ' is the angle between the incident beam direction and the normal to the surface. In accordance with the definition of spectral directional absorbing ability (see equation (6.26)), the quantity of radiation energy absorbed by the surface area unit per unit time, within a unit frequency band, can be presented as follows:

$$\mathrm{d}E_\nu = \alpha_\nu(\mathbf{r}, \nu, T, \mathbf{\Omega}', \ldots) I_\nu(\mathbf{r}, \mathbf{\Omega}')\cos\theta'\,\mathrm{d}\Omega'. \tag{7.11}$$

If the surface is supposed to be opaque, i.e. it absorbs and reflects the radiation, then the energy of absorbed radiation will be equal to the difference between the incident radiation energy and reflected radiation energy

$$\mathrm{d}E_\nu = I_\nu(\mathbf{r}, \mathbf{\Omega}')\cos\theta'\,\mathrm{d}\Omega' - \rho_\nu(\mathbf{r}, \mathbf{\Omega}' \to 2\pi) I_\nu(\mathbf{r}, \mathbf{\Omega}')\cos\theta'\,\mathrm{d}\Omega'. \tag{7.12}$$

Substituting (7.11) into (7.12), we obtain the relation between the directional absorbing ability and the directional-hemispherical reflectivity as:

$$\alpha_\nu(\mathbf{r}, T, \nu, \mathbf{\Omega}') = 1 - \rho_\nu(\mathbf{r}, \mathbf{\Omega}' \to 2\pi). \tag{7.13}$$

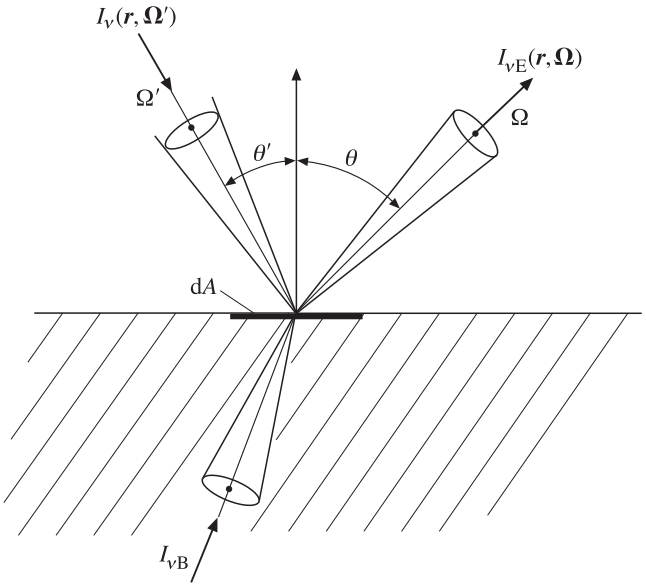

Figure 7.2. Schematic beam representation of the emitted, incident and reflected radiations for the determination of effective emission.

The latter characteristic is related, in its turn, in an integral manner with the reflection indicatrix (7.5).

If the investigated medium is at a state of local thermodynamic equilibrium (see section 4.4), and the Kirchhoff law (6.28) is satisfied, then the latter expression can be written in the following form:

$$\kappa_\nu(\mathbf{r}, T, \nu, \mathbf{\Omega}) = 1 - \rho(\mathbf{r}, \mathbf{\Omega} \to 2\pi). \tag{7.14}$$

Here it should be emphasized that the directional-hemispherical reflectivity should be considered from that direction where the observation with an instrument is carried out (in accordance with the Kirchhoff law).

The intensity of monochromatic effective radiation $I_{\nu E}(\mathbf{r}, \mathbf{\Omega})$ of an opaque surface element in the observation direction $\mathbf{\Omega}$ will be equal to the sum of intensities of thermal and reflected radiation (Figure 7.2). This is due to the fact that stochastic processes are independent, and their intensities can be summed. If the surface is at temperature T and has spectral emissivity $\kappa(\mathbf{r}, \mathbf{\Omega})$, then the intensity of thermal radiation will be determined by expression (6.30). As to the external radiation, it should be noted generally that the surface element is irradiated from all directions within the limits of a hemisphere, and the intensity of radiation, reflected by this element in the observation direction $\mathbf{\Omega}$, can be obtained according to relation (7.2). Thus, the total effective radiation from the surface element can be written as follows:

$$I_{\nu E}(\mathbf{r}, \mathbf{\Omega}) = \kappa_\nu(\mathbf{r}, \mathbf{\Omega}) I_{\nu B}(T, \nu) + \int_{\Omega'=2\pi} f_\nu(\mathbf{r}, \mathbf{\Omega}, \mathbf{\Omega}') I_\nu(\mathbf{r}, \mathbf{\Omega}') \cos\theta' \, d\Omega'. \tag{7.15}$$

The formula obtained is very widely used in remote microwave sensing practice, in quite different modifications, by the way. Here, as we have already noted, a serious problem is the adequate choice of a surface scattering model, i.e. the choice of function $f_\nu(\mathbf{r}, \mathbf{\Omega}', \mathbf{\Omega})$.

Now we consider two important cases, which are often used in microwave sensing practice: a surface with specular reflection and a surface with diffuse reflection. For a mirror surface the reflection indicatrix can formally be presented as a product of delta-function $\delta(\mathbf{\Omega} - \mathbf{\Omega}')$, that expresses the mirroring property of a surface, and the spectral power reflectivity from the direction $\mathbf{\Omega}' - R_{\nu\mathrm{P}}(\mathbf{\Omega}')$. The value of this reflectivity can be determined on the basis of the wave electromagnetic theory. Besides, we note, that the mirror surfaces possess the property of isotropy in the azimuthal direction. In this case the effective radiation of a unit surface can be written as a dependence on the polar angle (observation angle) θ only:

$$I_{\nu\mathrm{E}}(\mathbf{r}, \theta) = \kappa_\nu(\mathbf{r}, \theta) I_{\nu\mathrm{B}}(T, \nu) + R_{\nu\mathrm{P}}(\theta) I_\nu(\theta'). \tag{7.16}$$

A similar procedure, performed for the relation between the emissivity and reflectivity (7.14), makes it possible to obtain the following important expression:

$$\kappa_\nu(\mathbf{r}, \theta) = 1 - R_{\nu\mathrm{P}}(\mathbf{r}, \theta). \tag{7.17}$$

Comparing this expression with the electrodynamic solutions of the fluctuation–dissipation theorem (see section 4.3), we can easily see a complete analogy between expression (7.17), obtained from the energy conservation law, and the electrodynamic solution (4.20) for radiation of a semi-infinite space with a smooth boundary.

For diffusively emitting and reflecting surfaces quantities κ_ν and f_ν weakly depend on angles; as a result, the expression for effective radiation can be presented in a slightly different form (provided that the incident radiation does not depend on the direction):

$$I_{\nu\mathrm{E}}(\mathbf{r}, \mathbf{\Omega}) = \kappa_\nu I_{\nu\mathrm{B}}(T, \nu) + I_\nu \rho_\nu(2\pi \to \mathbf{\Omega}). \tag{7.18}$$

Here it is important to note that the external radiation will appear in a resulting radiation in a rather complicated manner. Whereas in the case of mirror surfaces, under conditions of real observations, there exist experimental techniques for separating out the information radiation component, which directly depends on the medium's properties, this procedure is much more difficult to perform for diffuse surfaces.

In the microwave band the relations presented above have usually been used in the terms of spectral brightness temperature of an investigated object $T_{\nu\mathrm{B}}(\mathbf{r}, \mathbf{\Omega})$, which, with regard to the Kirchhoff law (equation (6.30)) and relation (5.27), can be presented as

$$T_{\nu\mathrm{B}}(\mathbf{r}, \mathbf{\Omega}) = \kappa_\nu(\mathbf{r}, \mathbf{\Omega}) T_0, \tag{7.19}$$

where T_0 is the thermodynamic temperature of the investigated medium.

And, considering media with mirror boundaries possessing azimuthal isotropy properties, we can obtain the expression for effective spectral brightness temperature

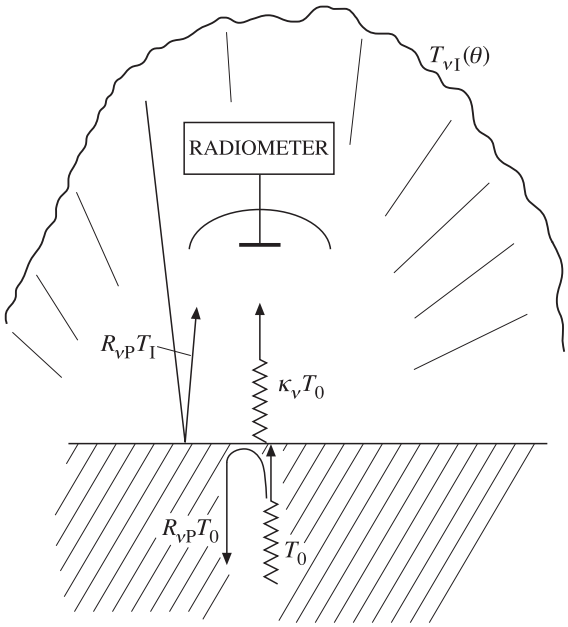

Figure 7.3. Schematic beam presentation of remote sensing measuring procedure. See explanations of notation in the text.

$T_{\nu BE}(\theta)$ with regard to the external brightness spectral integral illumination $T_{\nu I}(\theta)$ (sometimes called the firmament illumination)

$$T_{\nu BE}(\theta) = \kappa_\nu(\theta)T_0 + R_{\nu P}(\theta)T_{\nu T}(\theta). \tag{7.20}$$

The observational situation is illustrated schematically in Figure 7.3.

It should be noted that, unlike the IR band, in the microwave band the external brightness illumination varies in intensity within very wide limits – from 20–30 K up to 300 K – depending on the microwave working subrange and the state of cloudiness, and it also strongly varies depending on the observation angle (see Chapters 9 and 10).

In relation (7.20) the question is about spectral and differential (in angle) radiation characteristics of a medium. However, the total signal received by a radiometric system will depend both on the relationship between the angular characteristics of a studied object and the antenna system of a receiving device (see equation (5.28)), and on the amplitude-frequency characteristic of a receiving device (see equation (5.29)). We shall still be interested in the properties of physical media particularly; therefore, we shall further use relation (7.20), omitting for simplicity subscript ν. However, we shall always remember, that the question is about spectral characteristics.

Some important conclusions follow from relation (7.20). First, the brightness temperature of a physical medium, recorded by a remote instrument, is directly

related to the physical-chemical properties of a medium (via the emissive ability) and with its thermodynamic temperature. The spectral properties of a medium (for example, the dependence of its dielectric properties and, accordingly, of physical-chemical properties, on the working frequency) will also be displayed directly in spectral properties of the field of brightness temperature. Of importance here are the state and characteristics of the medium's boundary which, in their turn, have intrinsic and rather complicated spectral properties. The separation of volume and surface effects in a compound radiothermal signal is one of complicated problems of remote microwave sensing.

Second, since the emissivity of media, being under the conditions of local thermodynamic equilibrium, is less than unity (as a consequence of Kirchhoff's law), the brightness temperature of such media will always be lower, than the value of thermodynamic temperature of a medium (certainly, disregarding the firmament illumination). To restore the component, caused by physical-chemical properties, from the compound radiothermal signal, IR thermal remote measurements (along with radiothermal ones) of physical objects are usually applied. As a result, the information on a purely temperature field is obtained, and, then, the medium emissivity is restored. If it is indicated in such a manner that the medium emissivity exceeds unity, then, to a high probability, the radiation of a medium can be supposed to have a clearly non-thermal character (see section 4.4).

Third, to demonstrate the important role of brightness illumination, let us imagine mentally the following experiment. The investigated medium with an instrument are placed in a thermostat with emitting blackbody walls. In this case the brightness illumination temperature will not depend on the direction and will be equal to $T_{\mathrm{I}}(\theta) = T_0$. Substituting this value into (7.20) and making some transformations, we obtain that the effective brightness temperature will be equal to T_0 and will not depend on the physical properties of the medium. In other words, remote measurements, carried out under thermostatic control conditions, will not bear any information substance.

This can easily be confirmed by some other relationships as well. If we investigate two media with different emissivities (but with equal physical temperatures), then it follows from (7.20), that in observing these two media the radiobrightness contrast ΔT_{B} will be:

$$\Delta T_{\mathrm{B}} = (T_0 - T_{\mathrm{I}})\,\Delta\kappa. \tag{7.21}$$

It can be seen from this relation that, in spite of distinctions in physical properties of the media, determined as $\Delta\kappa = \kappa_1 - \kappa_2$, the measured radiobrightness contrast tends to zero as $T_{\mathrm{I}} \to T_0$. Under terrestrial atmosphere conditions such a situation takes place, for example, in the wavelength band of about 5 mm. Similar thermostated situations take place also in closed laboratory rooms, which makes it difficult to perform fine radiothermal measurements in such rooms.

Even earlier detailed onboard radiothermal experiments (1975–1979) have shown that the mirror component plays an essential part in forming the microwave effective radiation, even if the surface is optically rough. As an example, Figure 7.4 shows the fragments of radiothermal signal reception

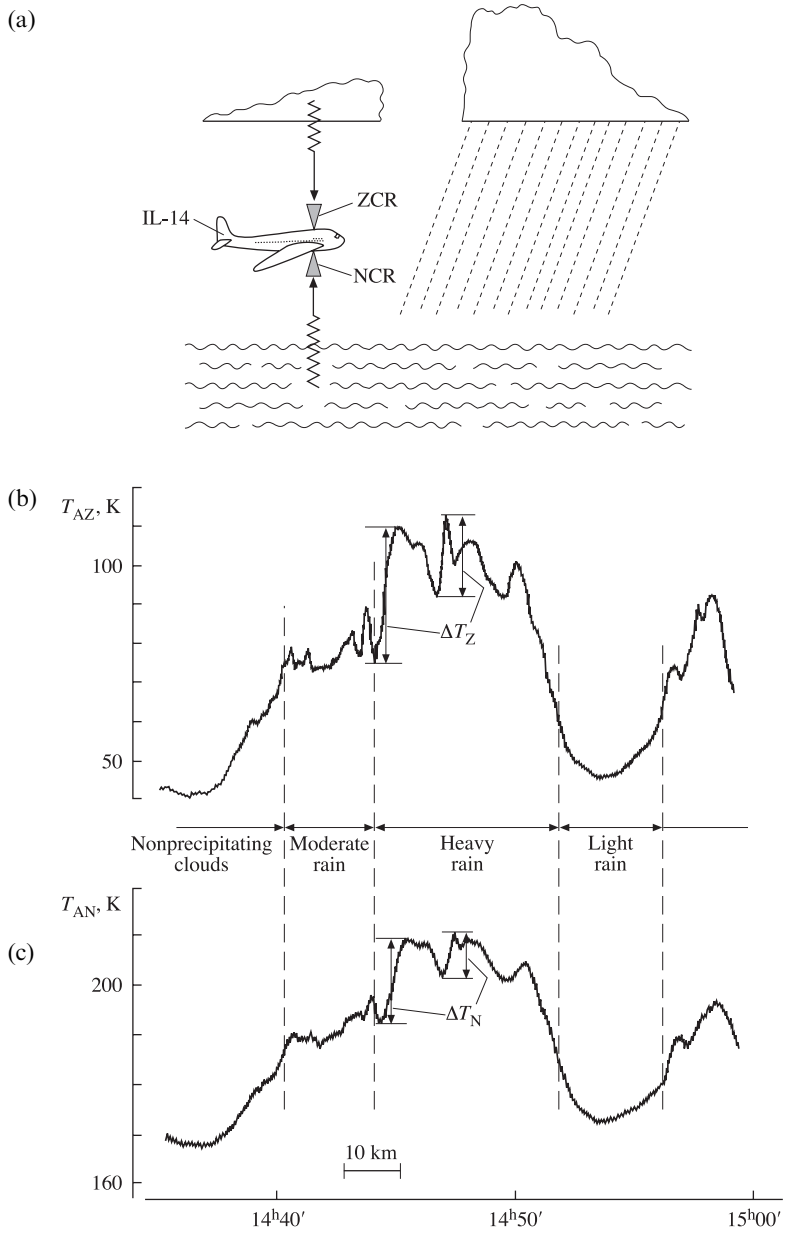

Figure 7.4. Remote microwave results of the specialized nadir-zenithal airborne (Russian IL-14) instruments (radiometer RNZ 0.8). The working area is the north part of the Caspian Sea on 22 April 1979. (a) Schematic presentation of measuring procedure. ZCh and NCh are the zenithal and nadir channels respectively. (b) and (c) are fragments of the radiometer output signal for zenithal channel T_{AZ} and nadir channel T_{AN}. Moscow time, spatial scale and indoor temperature calibration are shown on abscissa and on ordinate.

registrograms, obtained by means of a specialized onboard radiothermal device, which receives radiations simultaneously in the nadir mode (with respect to a flight vehicle) and in the zenith mode by two identical radiometers – zenithal instruments and nadir instruments. Specialized nadir-zenithal instruments of 8-mm band were manufactured and installed on the Russian IL-14 aircraft-laboratory by co-workers of the Space Research Institute of the Russian Academy of Sciences. The onboard experiments were carried out in the Caspian Sea area of water under complicated meteorological conditions, at strong sea surface disturbance and at low altitude of flight (200–400 m) (Figure 7.4(a)). The analysis of registrograms of nadir and zenithal channels (Figure 7.4(b), (c)) showed their virtually full identity from the viewpoint of variations of radiothermal peculiarities. Depending on precipitation intensity, the external illumination varies within very wide limits – from 40–50 K for a cloudy atmosphere up to 70–80 K – for precipitation of average intensity, and up to 100–110 K for hail showers. Accordingly, in the nadir channel the signal intensity varies from 170 K to 200–210 K. It should be noted, that it is virtually impossible to obtain such a detailed spatial structure of precipitation of various intensity by other techniques.

Proceeding from relation (7.20) and using the data of nadir T_N and zenithal T_Z channels, the first (and rather rough) estimation of sea surface emissivity can be given as:

$$\kappa \cong \frac{T_N - T_Z}{T_0 - T_Z}. \tag{7.22}$$

Substituting the values for various illumination intensities, we obtain the emissivity value for the disturbed sea surface as 0.51–0.53. This can also be done in another way, by considering the contrasts in the nadir (ΔT_N) and zenithal (ΔT_Z) channels' intensity from the same spatial peculiarity. In this case we have:

$$1 - \kappa = \frac{\Delta T_N}{\Delta T_Z}. \tag{7.23}$$

Substituting corresponding values of contrasts from the two channels (they are marked in Figure 7.4(b), (c)) for the same radiothermal peculiarity, we obtain the emissivity value as 0.51–0.52. It can be seen from this result that the estimates obtained by two methods – from the 'absolute' values and from contrasts – are very close. Thus, we can conclude that the use of a mirror model in interpreting radiothermal observations is quite justified, in the first approximation at least.

7.3 REFLECTION AND TRANSMISSION OF PLANE WAVES AT THE PLANE INTERFACE BOUNDARY

In the overwhelming majority of cases remote sensing practice deals with inhomogeneous media having rough boundaries. The full solution of the problem of radiation of such media is rather complicated. We shall consider some of the

problems in this book. For constructing complex models it is very useful to know the solutions of some simple problems, which, nevertheless, play a fundamental part. The simplest problem on wave propagation in the inhomogeneous medium is the problem of a plane monochromatic wave falling on a plane interface boundary of two media with different dielectric properties (the specular model of reflection). As is known, refracted (transmitted) and reflected waves arise in this case. Of importance here are the boundary conditions of the Maxwellian equations, which are presented not in the form of relation between the amplitudes of fields at the boundary (see equation (1.6)), but in the form of complex field reflectivities and transmissivities and (real) power reflectivities and transmissivities (Brekhovskikh, 1957; Veremey *et al.*, 1978; Finkelstein and Mendelson, 1980; Wilheit, 1978).

Let the interface boundary between two semi-infinite homogeneous media coincide with the plane $z = 0$ of the Cartesian coordinate system. The media disposed above ($z > 0$) and below ($z < 0$) the boundary are characterized by parameters $\dot{\varepsilon}_1$ and $\dot{\varepsilon}_2$, respectively ($\mu_1 = \mu_2 = 1$) (see section 1.6). To this boundary from the first medium falls a plane wave at angle θ_0 to axis z with circular frequency $\omega = 2\pi\nu$ and wave vector $\mathbf{k}_0 = k_1\mathbf{m}_0 (k_1 = (\omega/c)\sqrt{\dot{\varepsilon}_1}$, where $\mathbf{m}_0$ is the unit vector of the normal to the incident wave front) (see section 1.6). Then we make the plane of incidence that contains vector k_0 and axis z, coincident with the plane xz. We denote the wave vector of the reflected wave by $\mathbf{k}_1 = k_1\mathbf{m}_1$ and the wave vector of the transmitted wave by $\mathbf{k}_2 = k_2\mathbf{m}_2$; $\mathbf{n}_0$ is the unit vector of the normal to the interface boundary, directed from medium 2 to medium 1. According to (1.29) and (1.11), the electric and magnetic fields can be written as follows. For the incident wave:

$$\begin{aligned} \mathbf{E}_\mathrm{I} &= \mathbf{E}_0 \exp\left[\mathrm{j}k_1(\mathbf{m}_0\mathbf{r}) - \mathrm{j}\omega t\right] \\ \mathbf{H}_\mathrm{I} &= \frac{[\mathbf{m}_0\mathbf{E}_0]}{Z_1} \exp\left[\mathrm{j}k_1(\mathbf{m}_0\mathbf{r}) - \mathrm{j}\omega t\right] \end{aligned} \tag{7.24}$$

for the reflected wave:

$$\begin{aligned} \mathbf{E}_\mathrm{R} &= \mathbf{E}_1 \exp\left[\mathrm{j}k_1(\mathbf{m}_1\mathbf{r}) - \mathrm{j}\omega t\right] \\ \mathbf{H}_\mathrm{R} &= \frac{[\mathbf{m}_1\mathbf{E}_1]}{Z_1} \exp\left[\mathrm{j}k_1(\mathbf{m}_1\mathbf{r}) - \mathrm{j}\omega t\right] \end{aligned} \tag{7.25}$$

and for the transmitted wave:

$$\begin{aligned} \mathbf{E}_\mathrm{T} &= \mathbf{E}_2 \exp\left[\mathrm{j}k_2(\mathbf{m}_2\mathbf{r}) - \mathrm{j}\omega t\right] \\ \mathbf{H}_\mathrm{T} &= \frac{[\mathbf{m}_2\mathbf{E}_2]}{Z_2} \exp\left[\mathrm{j}k_2(\mathbf{m}_2\mathbf{r}) - \mathrm{j}\omega t\right]. \end{aligned} \tag{7.26}$$

Here $\dot{Z}_1$ and $\dot{Z}_2$ are the complex impedances of the first and second media (see equation (1.30)). To simplify the recording, we shall assume in this paragraph $\varepsilon_0 = \mu_0 = 1$. This condition will in no way influence the final result. At $z = 0$ the boundary conditions should be satisfied, which are reduced to the requirement of continuity of tangential components of vectors $\mathbf{E}$ and $\mathbf{H}$ of the total wave field

(see equation (1.6)). Hence, at $z = 0$ the fields should satisfy the equations

$$\begin{aligned}
[\mathbf{n}_0\mathbf{E}_0]\exp[\mathrm{j}(\mathbf{k}_0\mathbf{r})] + [\mathbf{n}_0\mathbf{E}_1]\exp[\mathrm{j}(\mathbf{k}_1\mathbf{r})] &= [\mathbf{n}_0\mathbf{E}_2]\exp[\mathrm{j}(\mathbf{k}_2\mathbf{r})], \\
[\mathbf{n}_0[\mathbf{m}_0\mathbf{E}_0]]\exp[\mathrm{j}(\mathbf{k}_0\mathbf{r})] + [\mathbf{n}_0[\mathbf{m}_1\mathbf{E}_1]]\exp[\mathrm{j}(\mathbf{k}_1\mathbf{r})] &= \frac{Z_1}{Z_2}[\mathbf{n}_0[\mathbf{m}_2\mathbf{E}_2]]\exp[\mathrm{j}(\mathbf{k}_2\mathbf{r})].
\end{aligned} \tag{7.27}$$

Since relations (7.27) should be satisfied at all points of the plane $z = 0$ (the condition of homogeneity of the plane boundary), this gives rise to the requirement of identical dependence of the fields of all three waves on coordinates x and y at $z = 0$. Therefore, the phase multipliers in the exponents should be identical and, hence,

$$k_1 \sin\theta_0 = k_1 \sin\theta_1 = k_2 \sin\theta_2. \tag{7.28}$$

This results in the well-known law of reflection for specular boundaries:

$$\theta_0 = \theta_1, \tag{7.29}$$

and in Snell's law for angles of incidence and transmission:

$$k_1 \sin\theta_0 = k_2 \sin\theta_2. \tag{7.30}$$

Note that here the question is about the complex values of both angles and amplitudes of wave vectors.

To determine the amplitudes of reflected and transmitted waves and, accordingly, the complex reflectivities and transmissivities, we turn to the system of equations (7.27). In this case we shall consider the waves of two different linear polarizations: the horizontally polarized wave with vector $\mathbf{E}$ perpendicular to the plane of incidence ($E_x = E_z = 0, E_y \neq 0$), and the vertically polarized wave with vector $\mathbf{E}$ lying in the plane of incidence ($E_y = 0, E_x \neq 0, E_z \neq 0$). A wave with arbitrary elliptical polarization can be obtained as a linear combination of these two solutions. In the first case, for the wave with horizontal polarization, we obtain from (7.27) the equations for unknown amplitudes E_1 and E_2

$$\begin{aligned}
E_0 + E_1 &= E_2, \\
\frac{1}{Z_1}(E_0\cos\theta_0 - E_1\cos\theta_0) &= \frac{1}{Z_2}\cos\theta_2.
\end{aligned} \tag{7.31}$$

Solving (7.31), we find the complex Fresnel coefficients, which relate the amplitudes of reflected and transmitted waves to the amplitude of an incident wave, i.e. the reflectivity and transmissivity:

$$\dot{R}_{\mathrm{H}12} = \frac{E_1}{E_0} = \frac{Z_2\cos\theta_0 - Z_1\cos\theta_2}{Z_2\cos\theta_0 + Z_1\cos\theta_2} = |\dot{R}_{\mathrm{H}12}|\exp(\mathrm{j}\varphi_{R\mathrm{H}}), \tag{7.32}$$

$$\dot{t}_{\mathrm{H}12} = \frac{E_2}{E_0} = \frac{2Z_2\cos\theta_0}{Z_2\cos\theta_0 + Z_1\cos\theta_2} = |\dot{t}_{\mathrm{H}12}|\exp(\mathrm{j}\varphi_{t\mathrm{H}}). \tag{7.33}$$

For the vertically polarized wave the calculation is more convenient to perform for vector $\mathbf{H}$, which is perpendicular to the plane of incidence in the given case. The

calculations, completely similar to those made above, lead to the expressions:

$$\dot{R}_{V12} = \frac{H_1}{H_0} = \frac{Z_1 \cos\theta_0 - Z_2 \cos\theta_2}{Z_1 \cos\theta_0 + Z_2 \cos\theta_2} = |\dot{R}_{V12}| \exp(j\varphi_{RV}), \tag{7.34}$$

$$\dot{t}_{V12} = \frac{H_2}{H_0} = \frac{2Z_2 \cos\theta_2}{Z_1 \cos\theta_1 + Z_2 \cos\theta_2} = |\dot{t}_{V12}| \exp(j\varphi_{tV}). \tag{7.35}$$

Some more important conclusions follow from relations (7.32)–(7.33) and (7.34)–(7.35), namely: by using the method of permutation of indices and summation, we obtain the relations between the reflectivities above R_{12} and below R_{21} the boundary and the reflectivities and transmissivities (for any polarization):

$$\dot{R}_{12} = -\dot{R}_{21}, \tag{7.36}$$

$$1 + \dot{R}_{12} = \dot{t}_{12}, \tag{7.37}$$

$$1 - \dot{R}_{21} = \dot{t}_{21}. \tag{7.38}$$

These relations are sometimes called the impedance form of boundary conditions.

In microwave sensing theory and practice the power reflectivities and transmissivities (or the coefficients in power) are often used. Their physical meaning is related to the active energy transfer by the electromagnetic field in media and between the media (through the boundary). The power reflectivities and transmissivities of the boundary of two media are defined as corresponding ratios of averaged values of the Poynting vector (see equation (1.20)):

$$R_{P12} = \frac{\bar{S}_1}{\bar{S}_0} = |\dot{R}_{12}|^2; t_{P12} = \frac{\bar{S}_2}{\bar{S}_0} = \frac{\mathrm{Re}\sqrt{\dot{\varepsilon}_2}}{\mathrm{Re}\sqrt{\dot{\varepsilon}_1}} |\dot{t}_{12}|^2. \tag{7.39}$$

The formulas are presented here for the condition of normal incidence of a plane wave on the interface boundary. The energy conservation law for the boundary of transparent (loss-free) media is usually formulated (Stratton, 1941) as a continuity of normal components of the total energy flux above the boundary and below the boundary:

$$\mathbf{n}_0(\bar{\mathbf{S}}_0 + \bar{\mathbf{S}}_1) = \mathbf{n}_0 \bar{\mathbf{S}}_2 \tag{7.40}$$

and this directly results in the relation we have repeatedly used before, namely,

$$R_{P12} + t_{P12} = 1. \tag{7.41}$$

However, more detailed investigations, carried out more recently (Veremey *et al.*, 1978; Finkelstein and Mendelson, 1980), have shown that for absorbing media the total energy flux is not generally equal to the sum of energy fluxes of partial waves. So, in determination of the energy conservation law we should use the energy flux of the total field (above the boundary), rather than the sum of components of energy fluxes. In such a statement (for the horizontal polarization) the energy conservation

law (the continuity of normal components of the flux of energy of the total field) can be written as follows:

$$\mathrm{Re}\,[(\mathbf{E}_0+\mathbf{E}_1)\{(\mathbf{H}_0\cos\theta_0)^*+(\mathbf{H}_1\cos\theta_1)^*\}]=\mathrm{Re}\,[\mathbf{E}_2(\mathbf{H}_2\cos\theta_2)^*]. \tag{7.42}$$

Here the power transmissivity at oblique incidence is equal to

$$t_{\mathrm{P}12}=\frac{(\mathbf{n}_0\bar{\mathbf{S}}_2)}{(\mathbf{n}_0\bar{\mathbf{S}}_0)}=\frac{\mathrm{Re}\,[\mathbf{E}_2(\mathbf{H}_2\cos\theta_2)^*]}{\mathrm{Re}\,[\mathbf{E}_0(\mathbf{H}_0\cos\theta_0)^*]}=\frac{\mathrm{Re}\,(\sqrt{\dot{\varepsilon}_2}\cos\theta_2)^*}{\mathrm{Re}\,(\sqrt{\dot{\varepsilon}_1}\cos\theta_0)^*}|\dot{t}_{12}|^2. \tag{7.43}$$

After some transformations we obtain from (7.39) the relations between power coefficients in the following form:

$$R_{\mathrm{P}12}+t_{\mathrm{P}12}=1+2|\dot{R}_{12}|\frac{\mathrm{Im}\,\sqrt{\dot{\varepsilon}_1}}{\mathrm{Re}\,\sqrt{\dot{\varepsilon}_1}}\sin\varphi_{12}, \tag{7.44}$$

where $\dot{R}_{12}=|R_{12}|\exp(-\mathrm{j}\varphi_{12})$. Such a relation takes place for the vertical polarization as well.

The above relation does not contradict the energy conservation law, since the additional term in the right-hand side is the result of superposition of incident and reflected fluxes and arising from the directional interference flux (the normal incidence) in the absorbing medium (Veremey *et al.*, 1978). If the medium from which the observation is performed is transparent (i.e. $\mathrm{Im}\,\sqrt{\dot{\varepsilon}_1}=0$), then we arrive at the former treatment of the energy conservation law (7.41), which shall be used hereafter.

7.4 POLARIZATION FEATURES OF RADIATION OF A GREY HALF-SPACE WITH A SMOOTH BOUNDARY

We shall use the results obtained above for considering the important problem of the radiation characteristics of a grey half-space with a smooth boundary. The simplified geometry of the problem is presented in Figure 7.5(a). The flight vehicle is in the medium 1 and observes the smooth surface at the polar angle of incidence θ. This angle is sometimes called a zenithal angle. In virtue of the properties of azimuthal isotropy of emission of smooth surfaces, all radiation characteristics do not depend on the observation azimuth. Since we consider an extended source (i.e. the solid angle of the antenna directivity pattern of an instrument is less than the solid angle of a radiation object), the value of a signal does not depend on the distance to an object (see equation (5.31), and, accordingly, the flight vehicle altitude over the studied surface has no significance.

Of principal importance here are the polarization characteristics of the emitting surface. The type of polarization of the received radiation will be determined by the polarization properties of the receiving instrument's antenna system. At present, there exists a great diversity of technological implementations of polarization measurements – from the reception of a purely linear polarization up to reception of polarizations rotating clockwise and counterclockwise. The appearance of complex types of polarizations is associated with the electromagnetic field interaction with

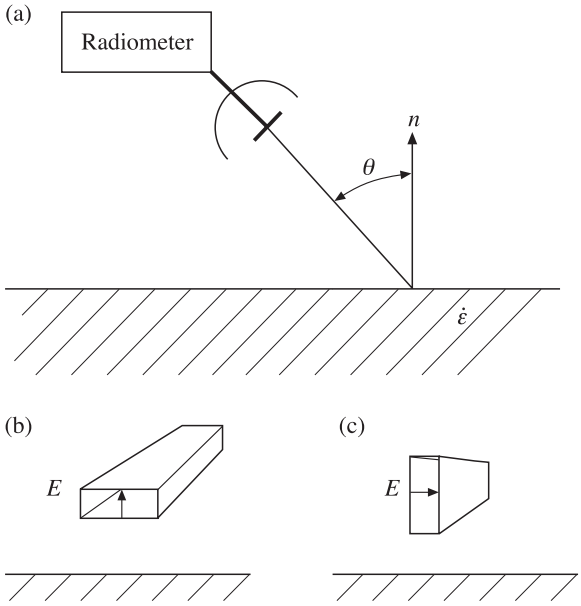

Figure 7.5. Schematic presentation of the remote sensing polarization procedure. (a) Cross-section in the plane of incident. (b) The reception of signal with vertical polarization by a waveguide horn-type antenna. (c) The reception of signal with horizontal polarization.

charged particles (the magnetosphere, the ionosphere). In our fairly simple case, of great significance is also the linear polarization of radiation, geometrically bound to the plane of interface. In this case the electromagnetic waves of two orthogonal polarizations can be distinguished: the horizontally polarized wave with vector **E** perpendicular to the plane of incidence and the vertically polarized wave with vector **E** lying in the plane of incidence.

With respect to the instruments this can be done rather simply – it is known that in the limited waveguides of transmission lines an infinite number of modes of oscillation can propagate, except the TEM mode which propagates in free space (see section 1.6). If, however, the relations between the values of geometric width (a) and height (b) of a waveguide (Figure 7.5(b), (c)) and the working wavelength are strictly fixed, the situation can be achieved where only one mode of oscillations propagates in the waveguide, this mode having the strictly defined direction of vector **E**, perpendicular to the wide wall of a waveguide. In this case the waveguide device plays the part of some kind of polarization filter, thus ensuring the reception of an electromagnetic wave of only one polarization. It can easily be seen that, when the long wall of a waveguide is parallel to the studied surface (Figure 7.5(b)), the reception of a vertically polarized electromagnetic wave will be accomplished. If the waveguide is turned through 90 degrees, when its narrow wall will be parallel to the studied surface, the mode of reception of a horizontally

polarized wave will be accomplished (Figure 7.5(c)). Certainly, it is important to take into account all these features when an antenna system is being installed on a flight vehicle. It is also important to take this into account when interpreting the observational data in the case of flight vehicle manoeuvring; for example, airplane pitch and roll manoeuvres can lead to significantly different results.

If we hypothetically imagine that a vehicle with an instrument is inside a semi-infinite isothermal medium, then in this case the instrument can be considered to be under conditions of thermostatic equilibrium. Thus, its readings will correspond to the value of thermodynamic temperature of the medium regardless of the direction of observation and of the polarization type.

Let us return to the values of Fresnel's coefficients (in the field) for two polarizations (equations (7.32)–(7.34)) and write them down in a simpler and more accessible form, which is often used in microwave sensing practice:

for horizontal polarization

$$\dot{R}_{\mathrm{H}} = \frac{\cos\theta - \sqrt{\dot{\varepsilon} - \sin^2\theta}}{\cos\theta + \sqrt{\dot{\varepsilon} - \sin^2\theta}} \tag{7.45}$$

and for vertical polarization

$$\dot{R}_{\mathrm{V}} = \frac{\dot{\varepsilon}\cos\theta - \sqrt{\dot{\varepsilon} - \sin^2\theta}}{\dot{\varepsilon}\cos\theta + \sqrt{\dot{\varepsilon} - \sin^2\theta}}. \tag{7.46}$$

In these expressions θ is the angle of observation in the external medium, and $\dot{\varepsilon} = \varepsilon_1 + \mathrm{j}\varepsilon_2 = \varepsilon_1(1 + \mathrm{tg}\delta)$ is the complex dielectric permeability of the medium studied and δ is the dielectric loss angle.

Since the boundary between media is smooth, then, using the model of specular boundary (see equation (7.17)), we can obtain the values of the medium's emissivity for two polarizations:

$$\kappa_i(\mathbf{r}, \theta, \dot{\varepsilon}) = 1 - |R_i(\mathbf{r}, \theta, \dot{\varepsilon})|^2, \tag{7.47}$$

where $i = h, \nu$.

Expressions (7.47) are very widely used in microwave sensing theory and practice, since they determine the fundamental basis in calculations and interpretation of more complicated models.

The full expressions for horizontal and vertical components of emissivity for a medium with arbitrary losses can be written as:

$$\kappa_{\mathrm{H}}(\theta) = \frac{4\sqrt{\varepsilon_1}\cos\theta\, A\cos(\psi/2)}{\cos^2\theta + \varepsilon_1 A^2 + 2\sqrt{\varepsilon_1}\cos\theta\, A\cos(\psi/2)}, \tag{7.48}$$

$$\kappa_{\mathrm{V}}(\theta) = \frac{4\sqrt{\varepsilon_1}\cos\theta\sqrt{1 + \mathrm{tg}^2\delta}\, A\cos(\delta - \psi/2)}{\varepsilon_1^2\cos^2\theta(1 + \mathrm{tg}^2\delta) + A^2 + 2\sqrt{\varepsilon_1}\cos\theta\sqrt{1 + \mathrm{tg}^2\delta}\, A\cos(\delta - \psi/2)}, \tag{7.49}$$

where $A = \sqrt{\left(1 - \dfrac{\sin^2\theta}{\varepsilon_1}\right)^2 + \mathrm{tg}^2\delta}$ and $\psi = \mathrm{arctg}\left[1 - \dfrac{\sin^2\theta}{\varepsilon_1}\right]^{-1} \mathrm{tg}\delta.$

7.4.1 Nadir measurements

In measurements at observation angles equal to zero (nadir measurements) the distinction between the vertical and horizontal polarizations disappears. The medium emissivity (with arbitrary losses) can be rewritten in a more compact form:

$$\kappa(0) = \frac{4\sqrt{\varepsilon_1 \cos\delta}\cos(\delta/2)}{\varepsilon_1 + 2\sqrt{\varepsilon_1 \cos\delta}\cos(\delta/2) + \cos\delta}. \tag{7.50}$$

For media with small losses (transparent media), i.e. for which $\mathrm{tg}\delta \to 0$, expression (7.50) can be even more simplified:

$$\kappa(0) = \frac{4\sqrt{\varepsilon_1}}{(\sqrt{\varepsilon_1}+1)^2}. \tag{7.51}$$

From this simple expression, nevertheless, follows a rather important conclusion: virtually all natural substances on the Earth possess emissivities whose values lie within some restricted region. So, it follows from consideration of Figure 7.6, which shows the dependences of emissivity on dielectric properties, that for transparent media the emissivity is limited to values ranging from 1, for media with $\varepsilon_1 \to 1$, to the value of 0.36, for media of fresh water type (for decimetre and metre wavelength bands; see Chapter 8). For transparent media with nonzero values of $\mathrm{tg}\delta$ expression

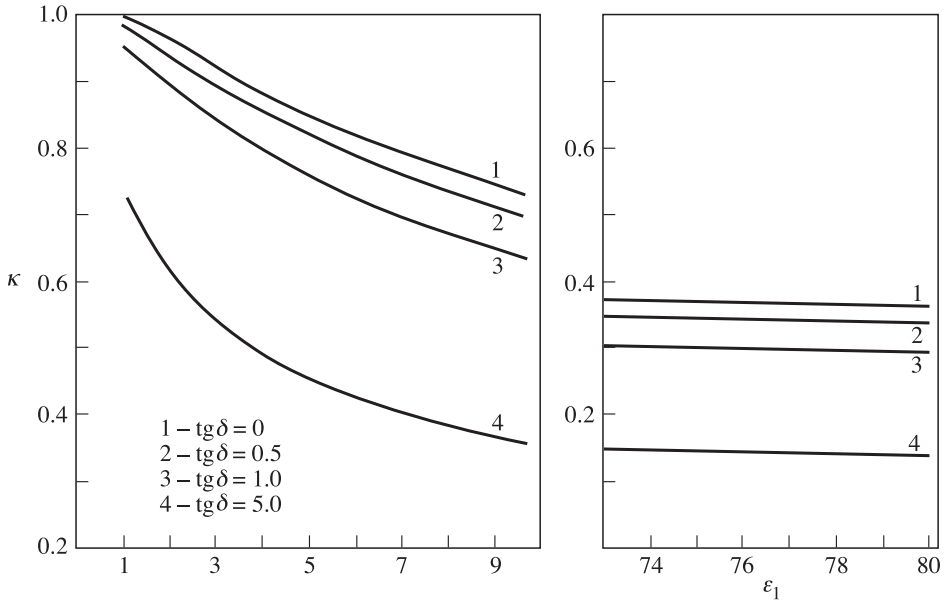

Figure 7.6. Emissivity of dielectric medium with smooth surface at nadir observation as a function of real relative dielectric constant (ε_1) at four values of loss angle tangent.

(7.50) can be expanded in a power series of δ, and we obtain the analytical form of dependence of emissivity on parameter δ:

$$\kappa = \kappa_0 \left[1 - \tfrac{3}{8}\delta^2\right]. \tag{7.52}$$

It is interesting to note here, that the increase of losses in a medium (the increase of parameter δ) results in decreasing the value of the medium's emissivity. This dependence is not so strong, generally speaking. So, it can be seen from relation (7.52) that, for the emissivity to change (decrease) by 5%, the angle of losses should increase considerably – from nearly zero up to values of 0.13–0.15. This implies that the change of losses in a medium influences the value of emissive properties much less than the variations of the real value of dielectric constant. Note that the above conclusions concern the physical models of solid and liquid media exclusively. For gases the situation is radically different (see Chapter 11).

The set of dielectric characteristics illustrated in Figure 7.6 is, of course, for demonstration only, since the real and imaginary parts of dielectric permeability of real substances are rigidly interrelated by fundamental Kronig–Kramers relations, and they should not be selected completely arbitrarily, of course.

The revealed decrease in the value of emissivity of a semi-infinite medium with increasing losses seems, at first sight, a paradoxical violation of Kirchhoff's law. This is not the case, however. As we have seen in section 4.3, the radiation emitted from the medium is caused by that part of the equilibrium thermal energy of a semi-infinite space which did not undergo reflection (see equation (4.20)). Its intensity is associated with the reflective properties of the medium, which increase (though insignificantly) with increasing losses in the medium and, thereby, lower the value of emissivity.

7.4.2 Angular measurements

Historically, the first microwave instruments were of purely nadir type (Basharinov *et al.*, 1969, 1974; Bespalova *et al.*, 1976a; Amirkhanyn *et al.*, 1975). However, it became clear fairly quickly, that the polarization properties (i.e. the properties which are revealed in observation at angles which differ from the nadir) of composite surfaces play an important part (see, for instance, Ulaby *et al.*, 1981, 1982, 1986; Fung and Chen, 1981; Paloscia and Pampaloni, 1988). They make it possible to determine the type of a surface and its state, to distinguish the signals from the surface and from vegetation, and to determine the properties of dynamic surfaces (such as the disturbed sea surface, for example). Virtually all modern radiothermal (both aircraft- and space-based) instruments operate under conditions which make it possible to record the radiation of a studied surface at fixed angles and at two polarizations (or at their combination) simultaneously (see Chapter 14).

For transparent media (at $\mathrm{tg}\delta \ll 1$) the emissivities for the modes of horizontal and vertical polarizations can be written in a fairly symmetrical form:

$$\kappa_{\mathrm{H}}(\theta) = \frac{4\sqrt{\varepsilon_1}\cos\theta\sqrt{1-\dfrac{\sin^2\theta}{\varepsilon_1}}}{\cos^2\theta + \varepsilon_1\left(1-\dfrac{\sin^2\theta}{\varepsilon_1}\right) + 2\sqrt{\varepsilon_1}\cos\theta\sqrt{1-\dfrac{\sin^2\theta}{\varepsilon_1}}}, \tag{7.53}$$

$$\kappa_{\mathrm{V}}(\theta) = \frac{4\sqrt{\varepsilon_1}\cos\theta\sqrt{1-\dfrac{\sin^2\theta}{\varepsilon_1}}}{\varepsilon_1\cos^2\theta + \left(1-\dfrac{\sin^2\theta}{\varepsilon_1}\right) + 2\sqrt{\varepsilon_1}\cos\theta\sqrt{1-\dfrac{\sin^2\theta}{\varepsilon_1}}}. \tag{7.54}$$

Figure 7.7 presents the calculated values of emissivities for water surface and dielectric media, which are used for modelling fertile soils with different moisture content.

Since our original model of a specular surface was based on the solutions of Maxwellian equations in the plane waves mode, all polarization features, known from Maxwellian theory, will be equally reflected in the solutions obtained for the emissive characteristics of media with smooth boundaries (Stratton, 1941; Alpert *et al.*, 1953). Here we note, first of all, the principal difference in the behaviour of an angular dependence for horizontal and vertical polarization. Whereas the behaviour of the horizontally polarized emissivity does not have any features, emission with vertical polarization has a prominent maximum. From the Maxwell electrodynamics viewpoint, its origin can be explained simply enough: this is a zero

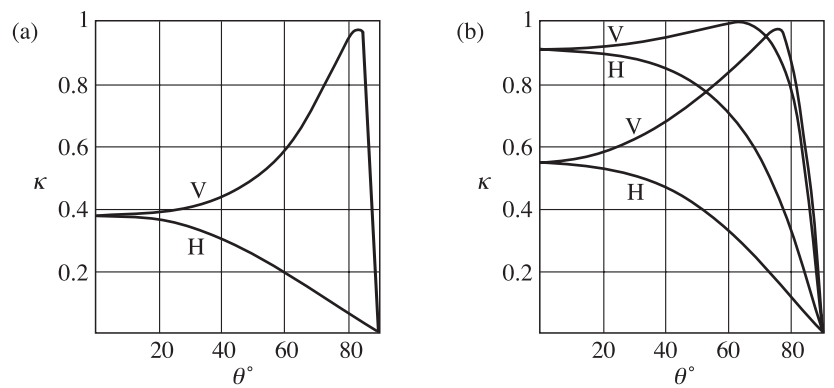

Figure 7.7. Polarization properties of emissivities of water surface and dielectric media. (a) Emissivity of water surface at 19°C as a function of the incident angle (zenith angle) for horizontal (H) and vertical (V) polarization at 10.5 GHz. (b) Emissivity of two dielectric media calculated with $\varepsilon = 3.5 + j0.1$ (upper curve) and $\varepsilon = 20 + j10$ (lower curve).

value of the Fresnel coefficient for vertical polarization at the Brewster angle (θ_{BR}). Equating the Fresnel coefficient value to zero (7.34), we obtain:

$$Z_1 \cos\theta_{BR} = Z_2 \cos\theta_2. \tag{7.55}$$

Taking the square of both parts of the equality and taking into account Snell's law for transparent media ($\mathrm{tg}\delta = 0$), we shall have, after some transformations:

$$\mathrm{tg}\theta_{BR} = \sqrt{\varepsilon_1}. \tag{7.56}$$

It is seen from this relation, that for pure dielectrics there exists the angle of incidence, called the Brewster angle, at which the incident wave passes to the second medium entirely (without reflections). From the thermal radiation viewpoint, the appearance of the Brewster angle can be interpreted as follows. When the Brewster angle appears, the wave resistance of an emitting medium becomes equal to the wave resistance of a vacuum, and the wave energy entirely escapes the medium where it was formed. In other words, at these angles and at vertical polarization the medium behaves as an ideal black body. It follows from (7.56) that for media with high values of dielectric properties ('cold' media in the radiothermal sense) the Brewster angle tends to 90° (for water, to 87–88°), whereas for media with a small dielectric constant value ('warm' media) the Brewster angle tends to 45° (Figure 7.7(b)).

Now we shall consider the variations of emissivity which can be related to a small deviation of angles at nadir investigations. These variations of angles are usually determined by features of a flight vehicle's manoeuvres. Expanding relations (7.53)–(7.54) into the Taylor series at $\theta = 0$ for small values of observation angles, we obtain:

$$\kappa_{VH}(\theta) = \kappa_0 \left[1 \pm \frac{\sqrt{\varepsilon_1} - 1}{\sqrt{\varepsilon_1} + 2} \frac{\theta^2}{2}\right], \tag{7.57}$$

where the plus sign relates to vertical polarization, and the minus sign to horizontal polarization. This fact suggests that the sensitive radiometric complex can behave as a device designed for detecting quite small inclines on a smooth surface. So, a surface incline of only 2° will result in quite a noticeable change of a radiothermal signal – by 2.5–3 K. The sign of the signal changing will be determined by the relation between the polarization plane of the instrument and the vector normal to the surface.

Now we shall consider the opposite situation: when the observation angle tends to 90°. For this purpose we introduce the complementary angle $\theta = 90° - \alpha$. This angle is sometimes called the grazing angle. Expanding relations (7.53)–(7.54) into the Taylor series of α, we obtain

$$\kappa_V(\alpha) \cong 4\sqrt{\varepsilon_1}\,\alpha; \kappa_H(\alpha) \cong \frac{4}{\sqrt{\varepsilon_1}}\alpha. \tag{7.58}$$

It can be seen from this relation that for natural media the vertical polarization value will always exceed the horizontal polarization values.

To understand the situation more clearly, we shall consider the following qualitative example (Figure 7.8). A flight vehicle with a radiometric receiver that

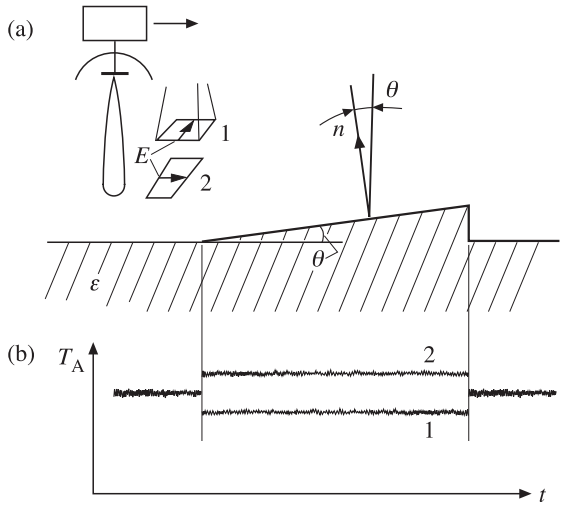

Figure 7.8. Schematic presentation of airborne remote sensing measuring procedure for the incline of a smooth surface with θ angle slope. 1, the reception of horizontal polarization; 2, vertical polarization. (a) Cross-section in the plane of incident. (b) Radiothermal signal registrations for horizontal (1) and vertical (2) polarizations.

measures two orthogonal polarizations approaches the incline of a smooth surface with slope θ (the cross-section is presented in Figure 7.8). When the vehicle is above the main surface, the observation is carried out in the nadir mode, and there is no distinction between two signals. When the vehicle reaches point x_1, the polarization geometry of observation sharply changes, because there arises the finite observation angle between the normal to the surface incline and the line-of-sight of the instrument's antenna, and, therefore, the difference in the signals of the polarization channels appears. Channel 1 will receive the horizontal polarization of radiation of the surface incline, and channel 2 the vertical one. Since the surface incline's slope is small, the variations of signals will be equal in magnitude and will differ in sign (equation (7.57)). As the vehicle turns through 90° around its axis, it is as if the channels change their places: channel 1 will receive the vertical polarization and channel 2 the horizontal one. When the vehicle escapes the incline observation zone at point x_2, the signals of the channels become equal again.

It can also easily be understood from the given geometry that in the case of flight vehicle manoeuvring (for example, when the aircraft engages in roll manoeuvres over a plane surface) the channels will give different results, i.e. channel 1 will receive the vertical polarization and channel 2 the horizontal one. When the aircraft performs pitching manoeuvres the channels will exchange places in their attribution to polarization measurements. Since the polarization sensitivity of a plane surface's emission to terrain the incline of which is quite high, this circumstance must be taken into account when interpreting observational data from flight vehicles performing various manoeuvres. So, a similar situation arises when observing the large-scale

surfaces of planets from spacecraft, which are in the permanent solar–stellar orientation mode (as, for example, the Russian automatic interplanetary station 'Mars-3' studying the large-scale surfaces of Mars). In such a case, during the orbital motion of the satellite the surface observation angle varies from 90° down to 10–15°. And, moreover, the roll angle γ between the plane of observation and the plane of vertical antenna polarization varies within the limit of 180°. It is clear that such mixed polarization regimes seriously hamper the interpretation of measurement results (Shapirovskaya, 1973).

Of interest is the fact that the first scanning radiothermal space instruments (for example, the ESMR instrument onboard 'Nimbus-5' (Allison *et al.*, 1974)) were designed in such a manner that the scanning mode be performed across the vehicle's route. As a result, each pixel (IFOV) in the scanning line was at its own observation angle, and, moreover, the spatial resolution varied 3–5 times. Under such conditions various zones of obtained radiothermal image have appeared in different polarization situations, which seriously hampered the interpretation of observations. This fact was quite quickly understood, and it was found inexpedient to use such a (transversal) scanning mode. Virtually all modern onboard radiothermal instruments apply a conical scanning mode, where each IFOV of the image is considered at a constant (and fixed) observation angle and in the fixed polarization mode (Chapter 14).

7.5 FEATURES OF EMISSION OF A TWO-LAYER STRUCTURE IN THE MONOCHROMATIC APPROXIMATION

Important special cases of layered media in the 'ocean–atmosphere' system are inhomogeneous structures of the 'film–water' type. They include such inhomogeneities on the ocean surface as disperse foam structures, layers of oil products on the sea surface, water–ice complexes (ice–water and water–ice), etc.

Let us consider in more detail the features of emission of such a structure, which consists of the plane-layered medium 2 on the backing produced from the semi-infinite medium 3. The observation is carried out from a vacuum – medium 1 with dielectric permeability $\varepsilon_1 = 1$. The expression for the monochromatic (i.e. considered under the assumption of an infinitely narrow passband of the receiving device) emissivity of a two-layered structure κ_{123} can be presented, using Kirchhoff's law, as follows:

$$\kappa_{123} = 1 - |\dot{R}_{123}|^2, \tag{7.59}$$

where $\dot{R}_{123}$ is the complex Fresnel coefficient a the two-layered medium when observing it from medium 1.

The calculation of this monochromatic Fresnel coefficient for a two-layered medium will be carried out using the method of summation of coherent partial beams, in just the same manner as is done in optics (Born and Wolf, 1999). Certainly, the use of such a monochromatic approach to thermal radiation problems (or, in other words, to noise radiation) requires theoretical and

experimental confirmation, which will be given in section 7.6. It is interesting to mention that, when earlier (at the beginning of the 1960s) experimenters made use of such an approach for interpreting the results of radiothermal measurements of the ice–water system (Tuchkov, 1968), this brought a sharply negative response from theorists. Nevertheless, the interference patterns in the thermal emitted radiation are a well-substantiated experimental fact now and have been actively used for solving a series of practical problems (Blinn *et al*. 1972; Glotov *et al*., 1975; Bespalova *et al*., 1978, 1983).

The geometry of the method of summation of partial beams is as follows (Figure 7.9): the plane wave falls on a two-layer structure with smooth boundaries at angle θ_1, is refracted in medium 2, passes through it and is reflected from the boundary with medium 3. Then this wave passes again through medium 2 and, being refracted at the upper boundary, escapes medium 2 at the same angle θ_1. By virtue of coherence with the basic primary wave, the escaping wave does have an impact. Since a part of energy will reflect from the upper boundary downwards to the boundary with medium 3, the whole cycle will be repeated again. The total retarding phase $\dot{\psi}$ in a medium with complex refraction index $\dot{n}$ is equal (see section 1.6) to:

$$\dot{\psi} = \dot{n}z/c_0 = \frac{2\pi}{\lambda_0}\dot{n}z. \tag{7.60}$$

Thus, the total retarding phase between the reflected primary beam and the beam that escaped medium 2, will be:

$$(AB + BC)\dot{n}_2\frac{2\pi}{\lambda_0} - AD\frac{2\pi}{\lambda_0}. \tag{7.61}$$

The following relations can easily be obtained from trigonometric considerations:

$$(AB + BC) = \frac{2h}{\cos\theta_2}; AD = 2h\,\mathrm{tg}\theta_2 \sin\theta_1. \tag{7.62}$$

Taking account of Snell's law in the form of $\dot{n}_2 \sin\theta_2 = \sin\theta_1$ and after some transformations the total retarding complex phase $\dot{\psi}$ can be presented as

$$\dot{\psi} = \frac{4\pi h}{\lambda_0}\dot{n}_2\cos\theta_2 = \frac{4\pi}{\lambda_0}\sqrt{\dot{\varepsilon}_2 - \sin^2\theta_1} = \alpha - \mathrm{j}\beta. \tag{7.63}$$

The total signal, obtained as a sum of interfered beams (this procedure is conventionally shown in Figure 7.9 as a collecting optical lens effect), represents an infinite series of relative complex amplitudes of partial beams:

$$\begin{aligned}\dot{R}_{123} &= \dot{R}_{12} + \dot{t}_{12}\dot{R}_{23}\exp(\mathrm{j}\dot{\psi}) + \dot{t}_{12}\dot{t}_{21}\dot{R}_{23}\dot{R}_{21}\dot{R}_{23}\exp(\mathrm{j}2\dot{\psi}) + \cdots = \\ &= \dot{R}_{12} + \dot{t}_{12}\dot{t}_{21}\dot{R}_{23}\exp(\mathrm{j}\dot{\psi})[1 + \dot{R}_{23}\dot{R}_{21}\exp(\mathrm{j}\dot{\psi}) + \cdots].\end{aligned} \tag{7.64}$$

Since the magnitude of product $|\dot{R}_{23}\dot{R}_{21}|$ is less than unity, the expression in square brackets is none other than the geometrical progression. Using the well-known expression for the sum of geometrical progression, as well as the impedance

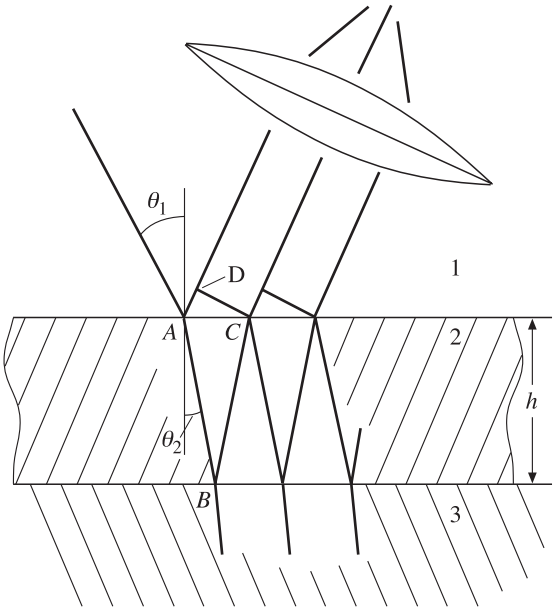

Figure 7.9. Reflections and transmissions of plane waves at the smooth boundaries of a two-layered structure. See the explanations of notation in text.

boundary conditions, we obtain the expression for the total coefficient of reflection from the two-layered medium:

$$\dot{R}_{23} = \frac{\dot{R}_{12} + \dot{R}_{23} \exp(\mathrm{j}\psi)}{1 + \dot{R}_{23}\dot{R}_{12} \exp(\mathrm{j}\psi)}. \tag{7.65}$$

Note that relation (7.65) can easily be generalized to the case of an isothermal multilayer structure, either by means of the impedance method (see section 7.7), or by means of the method of oriented graphs (Raev *et al.*, 1975). The study of prominently non-isothermal structures (i.e. structures with distinct gradients in the temperature field) was essentially more complicated for natural reasons (Klepikov and Sharkov, 1983, 1993; and see section 7.7).

Now we shall remain with the isothermal case and consider the situation where the film medium possesses small losses (the transparent medium with $\mathrm{tg}\delta \to 0$). This situation is fairly frequently encountered in sensing practice. In this case the emissivity of a two-layered medium can be written as:

$$\kappa = \frac{(1 - R_{12}^2)(1 - R_{23}^2)}{1 + R_{12}^2 R_{23}^2 + 2R_{12}R_{23}\cos(\psi + \varphi_{23})}, \tag{7.66}$$

where $\dot{R}_{23} = R_{23} \exp(\mathrm{j}\varphi_{23})$.

A new feature in emission of two-layered media consists in the presence of interference effects, which are related to the multiple reflection of plane

electromagnetic waves from the boundaries of media. The monochromatic emissivity of the total structure oscillates depending on the film depth, the period of oscillations, H, in the case of transparent (lossless) dielectric film being determined from (7.66) at $\delta_2 = 0$:

$$H = \frac{\lambda}{2\sqrt{\varepsilon_2 - \sin^2\theta}}. \tag{7.67}$$

The values of thicknesses for which the emission is maximum or minimum, are equal to:

$$h_{\max,\min} = \frac{\pi m - \varphi_{23}}{4\pi\sqrt{\varepsilon_2 - \sin^2\theta}}. \tag{7.68}$$

Here $m = 1, 2, 3, \ldots$ are integers, the emissivity maximum corresponding to odd m values and the emissivity minimum to even ones. It follows from (7.68) that for finite film thicknesses $h > 0$ the first extreme value of emissivity is a maximum $m = 1$, because, as can be shown for the oil–water system, the inequality $\pi > \varphi_{23}$ ($\varphi_{23} < 1$) takes place. In the case of other combinations of dielectric parameters (for example, the ice–ground structure) the first extremum of the $\kappa(h)$ dependence can be a minimum. This result is quantitatively confirmed by the $\kappa(h)$ dependences for ice–water and ice–ground structures (Figure 7.10). The electrophysical parameters of the media are indicated in Figure 7.10. Note that a thin film layer, some millimetres (3–5 mm) thick, can drastically change the emissive characteristics of a medium; so, the contrast of temperatures for water can exceed 100 K, and for ground 30 K. Note that the brightness temperatures of a structure are higher than the brightness temperature of a water surface (the structure is 'warmer' than the

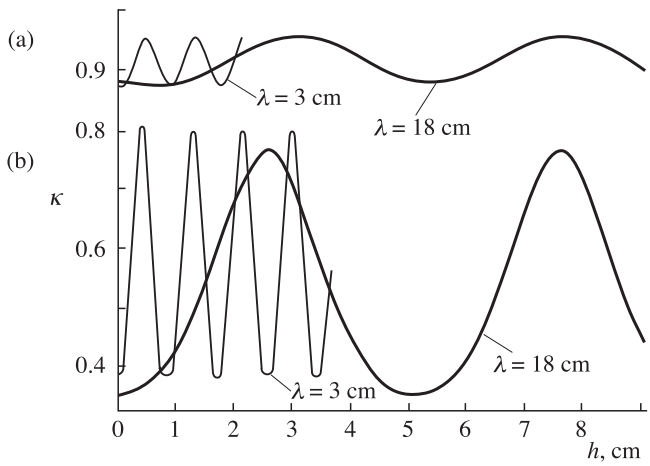

Figure 7.10. Relationships of emissivity of two-layered structures as a function of the ice depth. (a) Air–ice–soil structure; for ice $\varepsilon_1 = 3.2$; for soil $\varepsilon_1 = 12.5$ and $\mathrm{tg}\delta = 0.3$ (at 3 cm) and $\varepsilon_1 = 15$ and $\mathrm{tg}\delta = 0.07$ (at 18 cm). (b) Air–ice–water structure; see explanation of water data in Chapter 8.

backing). At the same time, for the ice–ground (or water–ice) structure the minimum temperature can be lower than the temperature of the ground (the structure is 'colder' than the backing).

The aforementioned effect with matching or mismatch influence of a film interlayer on the emission of a backing is similar, physically, to the antireflection effect or darkening effect in optics (Born and Wolf, 1999).

For small film thicknesses the contrast $\Delta T_B(h)$ can be approximated by the quadratic dependence on h:

$$\Delta T_B(h) = F(\lambda, \varepsilon_2)h^2, \tag{7.69}$$

where $F(\lambda, \varepsilon_2)$ essentially depend both on the wavelength, and on the dielectric properties of a film. The detailed calculations are presented in paper by Raizer *et al.* (1975b). The indicated dependence was experimentally confirmed in multifrequency remote studies of fields of thermal radiation of catastrophic oil spills in the Caspian Sea (Bespalova *et al.*, 1978).

It follows from the analysis of Figure 7.10 that the dielectric properties of a backing have no effect, virtually, on the period of oscillations $\kappa(h)$ (except a small 'phase' shift), which is determined by electrical properties of the film layer and radiation wavelength (7.67).

As the film thickness increases with finite losses, the interference effects weaken, and the contribution of natural thermal radiation of a layer is added. As a result, the $\kappa(h)$ quantity asymptotically escapes the radiation level, which is determined by the film's dielectric properties only. For a crude oil film with dielectric parameters $\varepsilon = 2.2 - j0.008$, quantity $\Delta T_B(h)$ will be constant only for $h > 1.4 \times 10^2 \lambda$. This results, for example, at the wavelength $\lambda = 0.8$ cm, in the layer thickness of about one metre. For more considerable losses in the film material, of the order of $\mathrm{tg}\delta \approx 0.1$–$0.2$, the interference pattern 'disappears' just at $(h/\lambda) \approx 1$–1.5. At the same time, for natural media with the tangent of the dielectric loss angle $\mathrm{tg}\delta \approx 10^{-3}$ the influence of losses in a medium for the first 4–5 oscillations at $(h/\lambda) \approx 1.5$ is virtually imperceptible.

Let us estimate the thickness of a film, for which it is possible to neglect the influence of small losses of oil, $\mathrm{tg}\delta \ll 1$, in determination of the radiobrightness temperature of an emitting surface. Taking into consideration that for $\mathrm{tg}\delta < 1$ and emission into the nadir $\beta \approx (2\pi h/\lambda)\sqrt{\varepsilon_2}\,\mathrm{tg}\delta$, we obtain addition to unity in the expansion $\exp(\pm\beta) \approx 1 \pm \beta$, which equals the value less than 0.01 and does not cause more than a 1% change in the emissivity value $\kappa(h)$. It follows from this result that for crude oils with characteristic dielectric parameters $\varepsilon_2 = 2.2$ and $\mathrm{tg}\delta = 3.6 \times 10^{-3}$ the influence of such losses on the considered radio-emission can be neglected (to an accuracy of 1%), provided that $h/\lambda < 0.3$.

The analysis of Figures 7.11 and 7.12, where the polarization dependences of the film–water structure are presented, indicates that the presence of a film of substance with other electrical parameters on the emitting surface drastically changes the polarization properties of the system as a whole. First, we note that for $h/\lambda > 1$ both at the vertical and (which is interesting to note) at the horizontal polarization 'pseudobrewster' angles appear, whose values, as well as the emissivity value, are

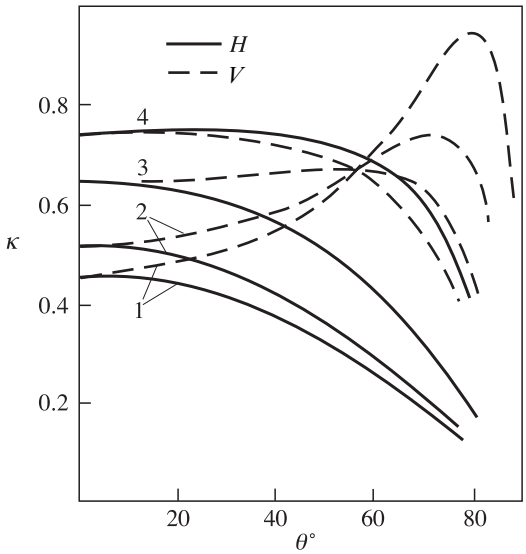

Figure 7.11. Polarization properties at 0.8 cm of oil sheet–water structure. For oil $\varepsilon_1 = 2.2$; $\mathrm{tg}\delta = 0$. For curves 1–4 oil sheet thickness is 0, 0.04, 0.08, 0.12 cm respectively.

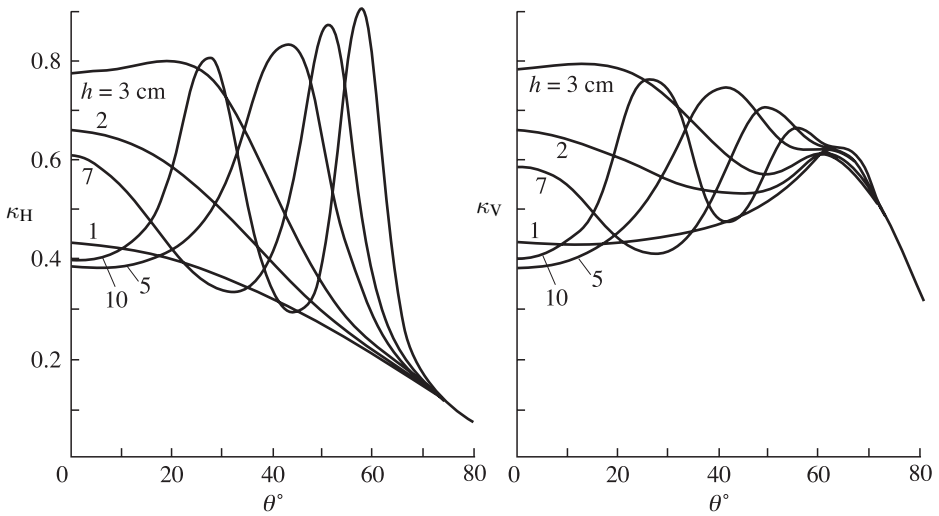

Figure 7.12. Polarization properties of air–ice–water structure. For ice $\varepsilon_1 = 3.2$, $\mathrm{tg}\delta = 0$; for fresh water $\varepsilon_1 = 44.78$, $\mathrm{tg}\delta = 0.95$. Ice sheet depths are shown by figures next to the curves.

rather sensitive to changes of the film thickness. So, when parameter h/λ changes by 20–30%, a qualitative rearrangement of the type of polarization characteristics can occur (Figure 7.12). The measurements of a horizontally polarized radio-emission component possess greatest sensitivity to film thicknesses up to 1 mm at observation

angles up to 40–50°. Second, in measurements of a vertically polarized radio-emission component at the Brewster angle for a film medium (under assumption of small losses, $\mathrm{tg}\delta \ll 1$) the emissivity does not depend on the film thickness and is determined by the emissivity of a clean surface of water.

Physically, this is related to a zero coefficient of reflection from the boundary of media 1–2 for a vertically polarized component of radiation at the Brewster angle $R_{V12}(\theta_{BR}) = 0$. Indeed, from (7.65) at $\mathrm{tg}\delta \ll 1$ and $\theta = \theta_{BR}$ we have (superscript 'V' is omitted hereafter):

$$\kappa_{123}(\theta = \theta_{BR}) = 1 - R_{23}^2(\theta_{BR}). \tag{7.70}$$

And, on the other hand, we can obtain the following relation between reflectivities for any components of polarization of a two-layered medium

$$\dot{R}_{23} = \frac{\dot{R}_{22} - \dot{R}_{13}}{\dot{R}_{12}\dot{R}_{13} - 1}. \tag{7.71}$$

From (7.71) for $R_{12}(\theta_{BR}) = 0$ we have $R_{23}(\theta_{BR}) = -R_{13}(\theta_{BR})$ and, further, with regard to (7.70), we have:

$$\kappa_{123}(\theta_{BR}) = \kappa_{13}(\theta_{BR}). \tag{7.72}$$

Thus, the vertically polarized radiation of the surface with a film is equal to the radiation of a clean surface at an angle which corresponds to the equality $R_{12}(\theta_{BR}) = 0$. This results in a curious experimental technique of determining the dielectric properties of a film coating. So, measuring the angular dependence of the brightness contrast between the clean surface and that covered with a film, $\Delta T_B(\theta)$, for a vertically polarized component of radio-emission, and determining angle θ_0, for which $\Delta T_B(\theta) = 0$, we can estimate the dielectric permeability of contamination as $\mathrm{tg}^2\theta_0 = \varepsilon_2$ (the well-known Brewster relationship). It follows from this relationship that in the region of $\varepsilon_2 = 1.78$–2.55 (which corresponds to basic types of widely used liquid oil products) the corresponding angle will be $\theta_0 = 54$–$58°$. It is obvious that the accuracy of determination of ε_2 by the proposed technique will be ± 0.15 units at an accuracy of the measured angle value of $\pm 1°$.

The characteristic form of spectral dependences for the 'matching' (or the 'antireflecting' optics version) case (i.e. when $\varepsilon_2 < \varepsilon_3$) is presented in Figure 7.13, and that for the 'mismatch' case ($\varepsilon_2 < \varepsilon_3$) in Figure 7.14. The latter version is interesting physically owing to the fact that the water film possesses wave resistance, which 'mismatches' the system, and the part of thermal radiation energy of the backing (the ice in the given case) is reflected 'backwards', which just explains the abnormally low brightness temperature of the system as a whole (Figure 7.14). As it would be expected, the dielectric properties of water play a decisive part in the given case and change both the values of emissivities and the form of frequency dependences; this influence becoming stronger with increasing wavelength (Figure 7.14).

Let us consider briefly the question of the solution of a reverse problem: the determination of electrical parameters and thickness from the data of radio measurements of thermal radiation of the film-backing system. Owing to the periodicity in $\kappa(h)$ dependence it is impossible, strictly speaking, to measure the film thickness with a one-frequency instrument. However, the use of n radio-frequency channels and the

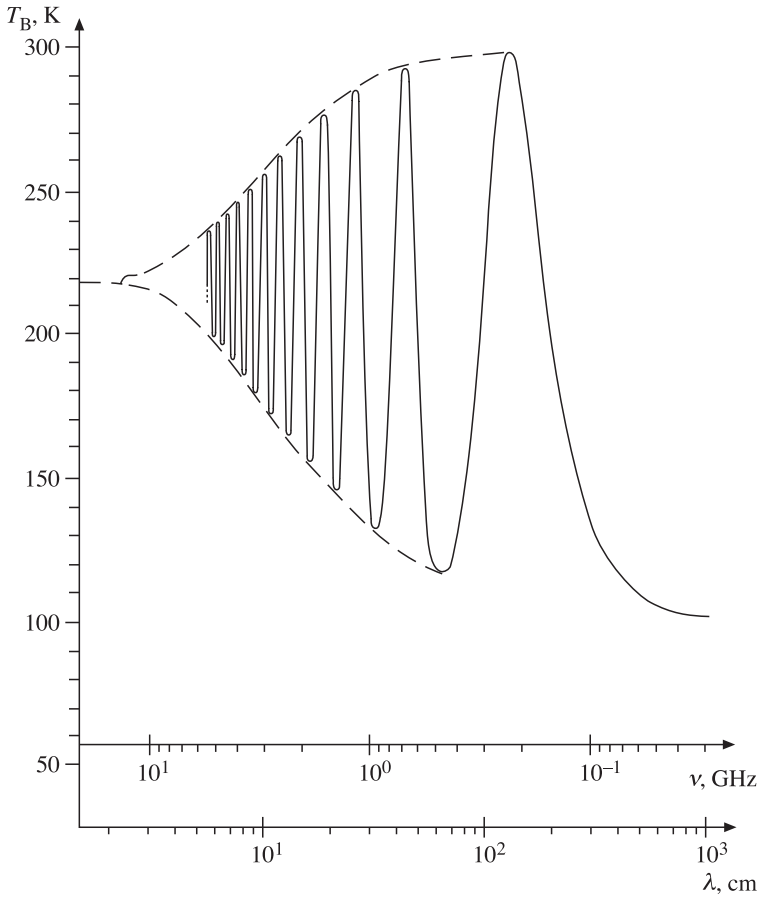

Figure 7.13. Spectral characteristics of the emission of an isothermal three-layered structure with nadir observation. For the second layer $\varepsilon_1 = 10$ and $\mathrm{tg}\delta = 0.04$; its depth is 10 cm. For the third layer $\varepsilon_1 = 100$ and $\mathrm{tg}\delta = 0.1$.

presentation of emissivity in the n dimensional space (at various wavelengths) makes it possible almost completely to avoid the uncertainty. Popov *et al.* (1976) have shown theoretically that the use of a three-dimensional image of emissivity for these purposes results, virtually, in a complete elimination of ambiguity. This has been experimentally confirmed for the first time in multifrequency remote studying of thermal emission fields of oil spreads in the Caspian Sea in 1976–1977 (Bespalova *et al.*, 1978). Detailed investigations (Raizer *et al.*, 1975b; Glotov *et al.*, 1975) of radiobrightness temperature gradients ΔT_B from parameters ε_2 and in the region of small thicknesses h have shown that in radiometric measurements of film thicknesses there exists an ambiguity of the order of 40–50%, caused by the absence of information on the true value of dielectric properties of a film. To estimate the latter value, polarization measurements (near the Brewster angle in a film) can be used.

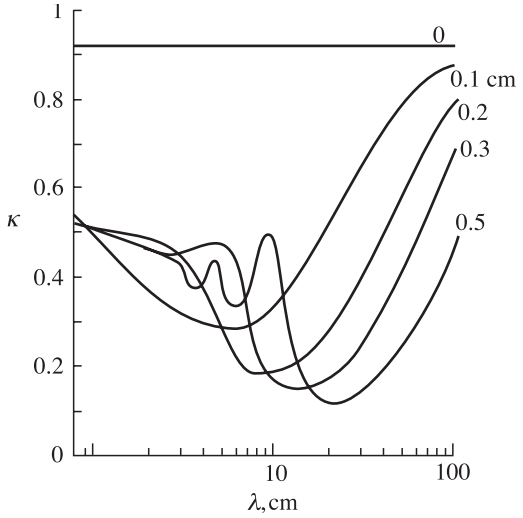

Figure 7.14. Spectral characteristics of the emission of air–water–ice structure with nadir observation. For ice $\varepsilon_1 = 3.2$; $\mathrm{tg}\delta = 0$. Spectral properties of water dielectric constants are specified by the Debye relaxation model (Chapter 8). Water sheet depths (cm) are shown by figures next to the curves.

7.6 PROPERTIES OF QUASI-COHERENCE IN THERMAL EMISSION AND THE LIMITS OF ITS APPLICABILITY

The interference patterns in thermal emission, revealed in previous sections, follow from the monochromatic approximation, i.e. they are obtained under assumption of an infinitely narrow passband of the receiving device. This feature of radiation represents, in essence, only an instrumental effect, since the interference as such arises 'inside' the receiving device because of the limited-in-frequency amplitude-frequency characteristic (AFC). This feature is not inherent in natural radiation as such. In addition, we note that the interference effects are most clearly revealed in the presence of pronounced dielectric boundaries in the natural structure (for example, a film of oil on the water surface). In the presence of smooth transition dielectric layers these effects are largely suppressed, however (section 7.7).

This effect – interference patterns in thermal emission – is considered in the present section, following Popov and Sharkov (1976), generally, for AFC of arbitrary form, and in more detail for the three most widespread special cases.

For greater physical clarity we shall consider the radio-emission of a very simple layered structure: the plane-parallel homogeneous layer 2, which covers a semi-infinite homogeneous medium 3. For simplifying derivations we shall assume the losses in media to be absent, that is, the dielectric permeabilities of considered media to be real. With allowance for these assumptions, the monochromatic (i.e. considered in the infinitely narrow frequency band) emissivity of a structure will take the form

(section 7.5):

$$\kappa(f) = \frac{(1 - R_{12}^2)(1 - R_{23}^2)}{1 + R_{12}^2 R_{23}^2 + 2R_{12}R_{23}\cos(2\pi f\tau)}, \tag{7.73}$$

where $\tau = (2h\sqrt{\varepsilon_2})/c$ is the delay time of a wave, reflected from the upper and lower boundary of a layer, with respect to the wave passed into a layer; R_{21} and R_{32} are the Fresnel coefficients for corresponding interface surfaces of media; h is the thickness of layer 2; c is the speed of light in vacuum; and $f = \nu$ is the frequency. It follows from (7.73) that the dependence of κ on the frequency and on the layer thickness has an oscillating character. It is important to note that the amplitude of oscillations is constant in the absence of losses in a layer.

The thermal emission of heated bodies of arbitrary geometrical shape is a random process with a virtually uniform 'white' spectrum of brightness temperature in the radio-frequency band and delta-correlated values of intensity of electrical and magnetic fields (Chapter 6).

The high-frequency channel (ahead of a square-law detector) of a receiving radiometric system restricts the spectrum as a result of received noise radiation of an intrinsic (power) AFC $G(f)$, thus establishing correlation link between instantaneous values of a noise output signal with nonzero correlation time $\tau_0 = 1/\Delta f$, where

$$\Delta f = \frac{1}{G_{\max}} \int_{\Delta f} G(f)\,\mathrm{d}f$$

is the effective passband width of the microwave channel of the radiometer (Chapter 3).

The radiobrightness temperature of an isothermal two-layered structure, measured by a radiometer that is medium 1 (in the absence of external illumination of the atmosphere and firmament), is equal to

$$T_{\mathrm{B}} = \kappa_{\Sigma} T_0, \tag{7.74}$$

where T_0 is the thermodynamic temperature of the total structure and κ_{Σ} is the emissivity averaged over the effective band of transmitted frequencies of a radiometer:

$$\kappa_{\Sigma}(\tau) = \frac{1}{G_{\max}\,\Delta f} \int_{\Delta f} \kappa(f) G(f)\,\mathrm{d}f. \tag{7.75}$$

It can be seen from this relation that the monochromatic approximation (7.73) quite well describes the measured emissivity of a layered structure only in the presence of a narrowband radiometric device. It is clear that the narrowband condition has the form of $\Delta f \ll 1/\tau$, where τ is the delay time between plane waves in a two-layered system (see section 7.5). Or, in other words, the delay time between plane waves is much less than the correlation time of a receiving system $\tau \ll \tau_0$. One of the methods for increasing the sensitivity of radiometric systems consists in extending the band of transmitted frequencies (Chapter 3). But, in this case, the greater the Δf the smaller the layer thicknesses for which the monochromatic approximation is valid. The violation of the band-narrowness condition results in decreasing the amplitude of

interference oscillations (which bear the useful information) down to their complete vanishing at $\tau \gg \tau_0$. Therefore, for high values of Δf and τ the calculation of the emissivity of a layered structure should be carried out by formula (7.75). However, the direct integration of (7.75) results in quite cumbersome expressions, even in the case of the simplest form of AFC functions. And for complicated AFC forms it even becomes impossible to derive accurate analytical expressions for emissivity κ_Σ. In this connection, it is of interest to derive simple approximate formulas for performing analytical consideration.

The mathematical approach described below, which was offered by Popov and Sharkov (1976), can be useful not just in considering thermal radio-emission of layered structures. This is because physically similar effects of interference of noise signals with a limited spectrum take place in optical systems and in transmission lines as well (Born and Wolf, 1999; Bulatov *et al.*, 1980).

The function of frequency $\kappa_\Sigma(f, t)$, appearing in expression (7.75), is an even, periodic and differentiable function of delay time τ and can be expanded in the Fourier series in cosines:

$$\kappa(f, \tau) = \frac{a_0}{2} + \sum_{n=1}^{\infty} a_n \cos(2\pi f n \tau). \tag{7.76}$$

Substituting expansion (7.76) into formula (7.75) and interchanging summation and integration, we obtain:

$$\kappa_\Sigma(\tau) = \frac{a_0}{2} + \frac{1}{\Delta f} \sum_{n=1}^{\infty} a_n \int_0^{\infty} G_0(f) \cos(2\pi f n \tau)\, \mathrm{d}f. \tag{7.77}$$

The integrals in the right-hand side of (7.77) present the Fourier transforms for AFC of a radiometer's $G_0(f)$; $G_0(f) = G(f)/G_{\max}$. Since the spectrum of received radiation is supposed to be 'white', function $G_0(f)$ is the spectrum of power of an output (after the high-frequency part of a radiometer) signal, and its Fourier transform, according to the Wiener–Khinchin theorem, is equal to the autocorrelation function of an output signal. That is, (7.77) can be written as:

$$\kappa_\Sigma(\tau) = \frac{a_0}{2} + \frac{1}{\Delta f} \sum_{n=1}^{\infty} a_n Q(n\tau), \tag{7.78}$$

where $Q(n\tau)$ are the values of the autocorrelation function of a noise output signal of a radiometer, corresponding to the shift in time by $n\tau$. Accordingly, the nth term of series (7.78), as well as of series (7.76), relates to the nth beam, which issues from the structure after n reflections from the lower boundary of layer 2. Therefore, the argument of the autocorrelation function in the nth term of series (7.78) is equal to $n\tau$, the delay time of the nth beam. As n grows, the Fourier coefficients a_n and the values of the autocorrelation function $Q(n\tau)$ tend to zero, owing to which series (7.78) rapidly converges for not too small τ values.

Let us estimate the behaviour of $\kappa_\Sigma(\tau)$ dependences for three AFCs of various form, which are most widespread in the practice of radiometric receiving systems

(see Chapter 3):

(a) rectangular type

$$G_0^{\mathrm{R}}(f) = \begin{cases} 1 & f_1 < f < f_2 \\ 0 & f < f_1; f < f_2, \end{cases} \tag{7.79}$$

(b) of resonance circuit type (sometimes called Lorentz's; see Chapter 2)

$$G_0^{\mathrm{L}}(f) = \frac{1}{1 + 4\left(\dfrac{f - f_0}{\Delta f}\right)^2}, \tag{7.80}$$

(c) Gaussian

$$G_0^{\mathrm{G}}(f) = \exp\left\{-2.773\left(\frac{f - f_0}{\Delta f}\right)^2\right\}, \tag{7.81}$$

where Δf is the bandwidth at the level of 3 dB and f_0 is the central frequency of the system's passband.

For the rectangular AFC, expression (7.78) is transformed to the form

$$\kappa_\Sigma^{\mathrm{R}}(\tau) = \frac{a_0}{2} + \frac{1}{\pi \Delta f \tau} \sum_{n=1}^{\infty} \frac{a_n}{2} \cos(2\pi f_0 n\tau); \sin(\pi \Delta f n\tau), \tag{7.82}$$

for Lorentz's AFC, to the form

$$\kappa_\Sigma^{\mathrm{L}}(\tau) = \frac{a_0}{2} + \sum_{n=1}^{\infty} a_n \exp(-\pi \Delta f n\tau) \cos(2\pi f_0 n\tau), \tag{7.83}$$

and for the Gaussian AFC, to the form

$$\kappa_\Sigma^{\mathrm{G}}(\tau) = \frac{a_0}{2} + \sum_{n=1}^{\infty} a_n \exp\left\{-\frac{\pi \Delta f^2}{2.773} n^2 \tau^2\right\} \cos(2\pi f_0 n\tau). \tag{7.84}$$

And also, in all formulas:

$$\frac{a_0}{2} = \frac{(1 - R_{12}^2)(1 - R_{23}^2)}{1 - R_{12}^2 R_{23}^2}. \tag{7.85}$$

Owing to rapid convergence of the series (7.75) for not too small τ values in formulas (7.79)–(7.81), only the first two terms can be retained in a series. Then we obtain (after calculating coefficient a_1):

$$\begin{aligned} \kappa_\Sigma^{\mathrm{R}} &= \frac{a_0}{2}\left[1 - 2R_{12}R_{23}\frac{\sin(\pi \Delta f \tau)}{\pi \Delta f \tau}\cos(2\pi f_0 \tau)\right], \\ \kappa_\Sigma^{\mathrm{L}} &= \frac{a_0}{2}[1 - 2R_{12}R_{23}\exp(-\pi \Delta f \tau)\cos(2\pi f_0 \tau)], \\ \kappa_\Sigma^{\mathrm{G}} &= \frac{a_0}{2}\left[1 - 2R_{12}R_{23}\exp\left\{-\frac{\pi^2 \Delta f^2}{2.773}\tau^2\right\}\cos(2\pi f_0 \tau)\right]. \end{aligned} \tag{7.86}$$

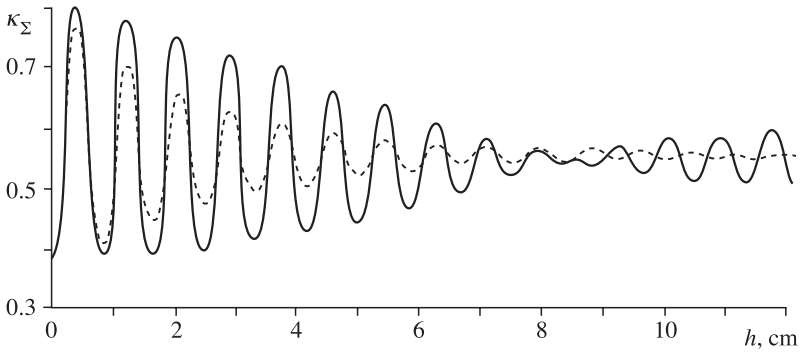

Figure 7.15. Relationships of two-layered medium (ice–water) emissivity averaged over the amplitude–frequency characteristic (AFC) versus ice depth with nadir observation at $T_0 = 273\,\mathrm{K}$; $f_0 = 10\,\mathrm{GHz}$, $\Delta f = 1\,\mathrm{GHz}$; for ice $\varepsilon_1 = 3.2$ and $\mathrm{tg}\delta = 0$; for water $\varepsilon_1 = 44.8$ and $\mathrm{tg}\delta = 0.95$. Continuous curve corresponds to a rectangular AFC; and dotted curve corresponds to a Lorentz-type AFC.

The formulas obtained indicate that the emissivity $\kappa_\Sigma(\tau)$ of a layered structure, averaged over AFC, oscillates with increasing layer thickness at the same period as the monochromatic one. However, unlike the monochromatic approximation, the oscillations attenuate in the given case, the attenuation being the faster the wider the frequency band. The envelope of oscillations is determined by the AFC form and represents, for the rectangular AFC, the function of type $\sin x/x$, for Lorentz's, $\exp(-x)$ and for the Gaussian $\exp(-x^2)$. The limit, to which the $\kappa_0(t)$ dependence tends for $\tau \to \infty$, does not depend either on the width or on the form of AFC, and coincides with the average-over-a-period value of the monochromatic dependence (7.73).

To estimate the accuracy of the approximate formulas obtained, numerical integration was carried out by computer, using accurate relations for the ice–water structure. Figure 7.15 presents the calculated dependences for the rectangular and Lorentz's AFCs. A similar curve for the Gaussian AFC differs from Lorentz's in one respect only: the amplitude of oscillations decreases more rapidly in this case. Formulas (7.86) qualitatively well describe the behaviour of these dependences; the maximum error, corresponding to the layer thickness $h \approx 0$, is less than 5% and rapidly decreases as h grows.

Let us compare the emissivity values of a layered structure, calculated by numerical integration, with the results of experiments (Blinn *et al.*, 1972). Figure 7.16 shows the dependences of the $T_\mathrm{B}(h)/T(\infty)$ on the thickness of a layer of sand on a metal backing. The form of AFC of the radiometric device used is not indicated in the authors' paper; however, the calculation shows that, among all AFC forms considered above, the rectangular one provides best agreement with the experiment. For comparison, Figure 7.16. gives the same dependence for the monochromatic approximation.

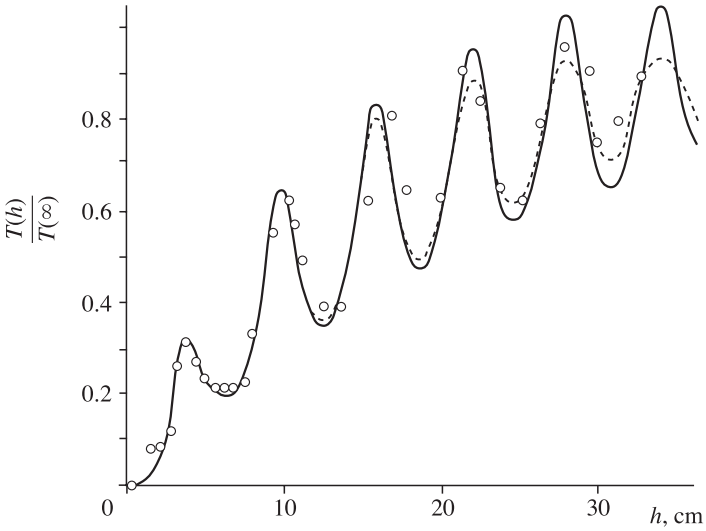

Figure 7.16. The ratio $T(h)/T(\infty)$ versus a layer depth for sand–metal plate structure with nadir observation, at $f_0 = 1.42\,\text{GHz}$, $\Delta f = 0.15\,\text{GHz}$; for sand $\varepsilon_1 = 2.95$ and $\text{tg}\delta = 0.05$. Continuous curve corresponds to monochromatic approximation; dotted curve corresponds to signal averaged over a rectangular AFC; circles correspond to experimental data by Blinn *et al*. (1972).

Note that similar complicated interference patterns usually accompany laboratory measurements of electromagnetic wave transmission through plane-layered objects (see, for example, Kohn, 1997).

The special analysis of dissipation in a film medium has shown (Raizer *et al*., 1975b), that the presence of losses in a layer makes attenuating of oscillations faster and slightly shifts them in phase, not involving any qualitative changes. Thus, the form and width of AFC of a radiometric system essentially influence the character of interference dependences at reception of thermal radio-emission of layered media and, therefore, the ultimate information capacity of microwave passive systems.

7.7 THERMAL EMISSION OF MULTI-LAYERED NON-ISOTHERMAL MEDIA

One major feature of radiothermal sensing methods is they may be used to obtain physical information about the internal structure of the medium studied. A whole class of boundaries between media (ice–water surface, dry and moist soil, soil–groundwater etc.) are classified, firstly by strong, non-uniform absorption (including in the vertical direction) and secondly by smooth variation of the physical characteristics in the media together with discontinuities and jumps in the

dielectric and thermal vertical profiles – in other words, situations where the scale of dielectric (or thermal) non-uniformity is comparable with the wavelength λ:

$$\left|\frac{\Delta\varepsilon}{\Delta z}\right| \geq \frac{\varepsilon}{\lambda}.$$

Problems of the electrodynamics of sharp non-uniform, strongly absorptive media are known to be very complicated, since they cannot be described adequately either in the framework of theory of radiative transfer or by classical approximations, for example, the WKB (Wentzel, Kramers, Brillouin) method (Levin and Rytov, 1967; Stogryn, 1970; Shulgina, 1975; Tsang *et al*., 1975).

Over a prolonged period a large variety of modifications of the plane-parallel model of microwave emission has been utilized without detailed analysis of the ranges of their feasibility (see, for instance, Tuchkov, 1968; Basharinov *et al*., 1968; Tsang and Kong, 1976; Wilheit, 1978; Bardati and Solimini, 1984).

In its fully completed form microwave emission theory was formulated by Klepikov and Sharkov in 1983 and developed in 1993 (Klepikov and Sharkov, 1983, 1993). The theory may be applied when describing emission in any irregular non-isothermic multi-layered media without restrictions, which are typical for previous modifications.

Klepikov and Sharkov performed a detailed theoretical study of the processes leading to the development of the natural radiation of highly non-uniform, non-isothermal, plane-stratified media with arbitrary variations of the dielectric and temperature-related parameters.

7.7.1 Physical substance of the problem

Kirchhoff's law, which relates the intensity of the radiation from a real medium to the radiation from an absolutely black body, may be used to determine the emissivity of a semi-infinite sphere using the energetic coefficient of reflection of an auxiliary plane wave from the interface between media (see Chapter 4 and section 7.4). This approach can only be applied correctly to isothermal media. On the other hand, use of the phenomenological radiation transfer equation (which describes the energy balance in a section of the medium) to calculate the thermal radiation of non-isothermal media is limited to cases of media with small losses and fairly smooth variations of the complex dielectric constant (see Chapter 9). In this case, all waves multiply-reflected in the medium, together with the corresponding interference effects, are neglected.

First attempts to consider thermal emission for the comparatively simple cases of two- and three-layered media with different temperatures were performed by Tuchkov (1968) and Basharinov *et al*. (1968). They used the method where direct and reflected energy fluxes are summed to obtain the expressions for brightness temperature that define the emission of a complete structure. Such a method did not take account of phase relationships for multiply-reflected waves and, hence, a number of important effects were neglected.

A rigorous solution to the problem of the thermal radiation of a non-uniform, non-isothermal medium may be obtained using electrodynamics fluctuation theory for thermal radiation, in which the relationship between the correlations of the external fluctuating fluxes and the thermodynamic temperature of the medium in equilibrium is determined by the fluctuation/dissipation theorem (FDT) (see Chapter 4). In the work of Stogryn (1970) the FDT and the solution of the wave equation for the propagation of waves in a non-uniform medium were used to obtain a second-order differential equation with two boundary conditions for the intensity of thermal radiation, and a quasi-classical approximation (WKB) was used to compute the brightness temperature for weakly non-uniform media. This solution actually takes account of the variation of the thermal radiation of individual areas of the medium with variations of the real part of their dielectric constant, but ignores interference effects. This process was developed in a paper by Shulgina (1975), where, in particular, it was shown that the solution obtained by the WKB method is a well-defined generalization of the phenomenological radiation transfer equation to the case of arbitrary absorption, since it takes account of the refraction of rays in an absorbing medium. The same paper also determined a condition for the applicability of the WKB method to non-uniform media in the form of an inequality

$$\left|\frac{\mathrm{d}\varepsilon}{\mathrm{d}z}\right| \ll \frac{2\pi}{\lambda}\varepsilon$$

(λ is the wavelength of radiation in free space, ε is the dielectric constant of the medium), which implies that the scale of the non-uniformity is large in comparison with the wavelength. For media with sharp variations of the dielectric parameters at distances comparable with the radiation wavelength, known solutions using the WKB method were not suitable.

An accurate closed-form solution of the problem of the thermal radiation from non-uniform, non-isothermal media has only been found for a number of smooth profiles of dielectric parameters and temperature. An example of such a solution for exponential profiles was given in work by Tsang *et al.* (1975). Because of the variety of possible types of vertical profiles of the parameters of media, including sharp changes of the latter, approximation methods are particularly important.

One such approach involves studying the radiation from a half-space with arbitrary vertical profiles of the complex dielectric constant and the temperature, in the framework of a model of a stratified medium. Based on the results of Stogryn (1970), the wave equation for waves in a stratified medium was solved in a paper by Tsang *et al.* (1975) using a Green function for a multilayered structure, and the intensity of the radiation for the whole medium was computed in the form of a sum of terms for each layer. The amplitudes of the direct and reflected waves from each layer were found, independently from the radiation problem, using a matrix method for the whole structure; this complicates physical interpretation and comparison with solutions obtained using other methods. An analogous problem in the work of Wilheit (1978) was solved by computing the energy functions for wave transmission from each layer to the surface, using an iterative method to satisfy the boundary conditions in each layer. However, here, interference

effects were calculated for the subcase in which the electric field vectors of the back waves are collinear, which only arises for radiation with a horizontal polarization.

In this section, we describe (following Klepikov and Sharkov, 1983, 1993) a method for analysing the thermal radiation from stratified, non-uniform, non-isothermal media for an arbitrary angle of observation and an arbitrary polarization type; this differs from previous work in that the expressions for the brightness temperature are derived in a sequence of stages, being deduced initially for a single layer bounded on both sides and then generalized to all the layers of the structure as a whole. In this approach, the closed-form nature of the final result provides for more complete identification of both the physical characteristics of the method used and the constraints on its applicability to the problem of the emission of non-uniform, non-isothermal media.

7.7.2 Thermal emission of non-isothermal media with arbitrary parameters

Let us consider a time-stationary, non-uniform, vertically non-isothermal, non-magnetic medium bounded by the plane xy and occupying the region $z < 0$. We shall assume that the medium is in local thermodynamic equilibrium, whence the scale of non-uniformities of the parameters of the medium is considerably greater than the radius of correlation of the fluctuating fluxes, and the radiation at each point of space is described by Planck's law. From physical considerations, it is clear that, for arbitrary constraints on the value of the profiles of the complex dielectric constant $\dot{\varepsilon}(z)$ and the temperature $T(z)$, for computation of the brightness temperature T_{br} with an arbitrary given accuracy, it is sufficient to consider a layer of finite thickness D, outside which the medium is assumed to be uniform and isothermal. In accordance with the model of a stratified medium, the layer D is divided into N planar layers of thickness d_j (not generally equal). In each layer, the dielectric constant $\dot{\varepsilon}_j$ and the temperature T_j are assumed to be constant and equal to the average values of $\dot{\varepsilon}(z)$ and $T(z)$ in the jth layer. Thus, the continuous profiles of the parameters of the medium are replaced by step functions. The legitimacy of this substitution and the consequent computational errors will be considered below (section 7.7.4).

Suppose that an auxiliary planar monochromatic wave $E = E_0 \exp(\mathrm{i}\mathbf{k}_0\mathbf{r})$ with wave vector $\mathbf{k}_0$ propagates from the upper half-space $\varepsilon = 1$ to the plan xy at an angle θ_0 to the normal to the medium interface, where λ is the wavelength in free space and

$$\mathbf{k}_0 = \frac{2\pi}{\lambda}\{\sin\theta_0, 0, \cos\theta_0\}. \tag{7.87}$$

The above assumption that the parameters of the medium are constant in each layer enables us, when computing the radiation intensity, to apply Kirchhoff's law to each layer individually. In this case, this reduces to determining the full absorption of the wave power by the planar layer, which is bounded on both sides, taking into account interference due to reflection from the boundaries.

Let us consider a wave propagating at an angle θ_j (in a medium with absorption, the angle of refraction is complex) in the layer of thickness d_j with given wave

reflection (Fresnel) coefficients (in terms of the amplitude of the electric field) R_j^+ and R_j^- within the layer from the upper and lower boundaries respectively, where E_{0j} is the amplitude of the electric field at the (internal) upper boundary of the layer and the wave vector $\mathbf{k}_j$ is:

$$\mathbf{k}_j = \frac{2\pi}{\lambda}\{\sin\theta_j, 0, \cos\theta_j\}\sqrt{\dot{\varepsilon}_j}, \tag{7.88}$$

where $\dot{\varepsilon}_j$ is the complex dielectric constant. In what follows, when we are considering an individual layer, we shall omit the index.

The full field of the wave layer, taking into account multiple reflection, consists of the sum of two infinite series of direct and multiply-reflected, non-uniform planar waves with amplitudes decaying in a geometrical progression; thus, this may be written in the form

$$E_\Pi(z) = E_0 \frac{\mathbf{h}^+ \exp(\mathrm{i}k_z, z) + \mathbf{h}^- \operatorname{Re}^{-\mathrm{i}k_z(z-d)}}{1 - R^+R^- \exp(-2\mathrm{i}k_z d)}, \tag{7.89}$$

where $\mathbf{h}^+$ and $\mathbf{h}^-$ are unit vectors corresponding to the direction of the vector of the electric field of the wave in the layer (with horizontal and vertical polarizations).

The density of full losses of the wave in the layer in the direction normal to the boundary is equal to the integral of the imaginary part of the complex Poynting vector over the whole thickness (Stratton, 1941):

$$\Pi = \frac{2\operatorname{Im} k_z}{E_0^2}\int_0^d |E_\Pi|^2 \,\mathrm{d}z, k_\mathrm{z} = k\cos\theta. \tag{7.90}$$

In accordance with the generalized law of Kirchhoff for the theory of radiation (with the condition $h\nu \ll kT$, where h and k are the Planck and Boltzmann constants (respectively) and ν is the radiation frequency, which is usually in the microwave band), the brightness temperature T'_{br} at boundary of the layer (on the internal side) has the form

$$T'_{\mathrm{br}} = \Pi T, \tag{7.91}$$

where T is the temperature of the layer.

By virtue of the statistical independence of the radiation of different layers, the brightness temperature on the surface of the medium is the sum of the brightness temperature of all the layers with weight coefficients $M_j = |E_{0j}/E_0|^2$, which characterize the attenuation of the power of the wave as it propagates from the corresponding layer to the surface, taking into account multiple reflection in all overlying layers

$$T_{\mathrm{br}} = \sum_{j=1}^{N} T_{\mathrm{br}} M_j = \sum_{j=1}^{N} \Pi_j T_j M_j. \tag{7.92}$$

Thus, the problem of determining the thermal radiation reduces to determining the transmission and reflection coefficients for a plane wave in a stratified medium. The wave characteristics of a multi-layered medium may be successfully determined using the tried and tested method of impedance characteristics, whereby the main equations may be written in the compact form of iterative equations. A detailed

description of the method, as applied to a stratified medium, was given by Klepikov and Sharkov (1983).

For the calculation of the brightness temperature from formula (7.92), taking into account (7.90), for a horizontally polarized wave, we have

$$T_{\text{brh}} = \sum_{j=1}^{N} \frac{T_j |W_j|^2}{|1 - R_j^- R_j^+ \exp(2\text{i}\psi_j)|^2} \left[(1 - \exp(-2\text{Im}\varphi_j))(1 + |R_j^- \exp(\text{i}\psi_j)|^2) + 4 \frac{\text{Im}\psi_j}{\text{Re}\,\psi_j} \text{Re}(R_j^- \exp(\text{i}\psi_j))(\text{Im}\exp(\text{i}\psi_j)) \right] \frac{\text{Re}\,Z_j}{\text{Re}\,Z_0} + T_{N+1} |W_{N+1}| \frac{\text{Re}\,Z_{N+1}}{\text{Re}\,Z_0}. \tag{7.93}$$

Similarly, for the vertical polarization, we have

$$T_{\text{brv}} = \sum_{j=1}^{N} \frac{T_j |W_j|^2}{|1 - R_j^- R_j^+ \exp(2\text{i}\psi_j)|^2} \left[(1 - \exp(-2\,\text{Im}\,\psi_j))(1 + |R_j^- \exp(\text{i}\psi_j)|^2) + 4 \frac{\text{Im}\,\psi_j}{\text{Re}\,\psi_j} \text{Re}(R_j^- \exp(\text{i}\psi_j)\,\text{Im}(\exp(\text{i}\psi_j)) \left(\frac{|k_{zj}| - k_x^2}{|k_j|^2} \right) \right] \frac{\text{Re}\,Z_j}{\text{Re}\,Z_0} + T_{N+1} |W_{N+1}|^2 \frac{\text{Re}\,Z_{N+1}}{\text{Re}\,Z_0}. \tag{7.94}$$

Both formulas implicitly involve the wave parameters and Z_j, R_j^+, R_j^- and W_j, depending on the polarization. The formulas are summed over all layers $j = 1, \ldots, N$. The index $j = N + 1$ describes the parameters of the uniform isothermal medium outside the layer D. W_j denotes the transmission coefficient (in terms of amplitude) from the internal side of the upper boundary of the layer j to the boundary of the medium, expressed in terms of input impedances Z_{in} as follows:

$$W_j = \prod_{m=1}^{j} \frac{Z_{\text{in}m-1}^+ + Z_{m-1}}{Z_{\text{in}m-1}^+ + Z_m}. \tag{7.95}$$

Since the component of the power of the total field of the wave normal to the boundary is conserved (see section 7.3), it is possible to determine the relationship between W_j and the coefficients M_j namely the attenuation of the wave power on transmission from the upper boundary of layer j to the surface of the medium:

$$M_j = |W_j|^2 = \frac{\text{Re}\,Z_j}{\text{Re}\,Z_0}. \tag{7.96}$$

The index '0' relates to the region observed, namely the free space. Since the conversion to the energy characteristics of the propagation of waves in stratified media only takes place after the amplitude of the field in free space has been found, the calculation is not complicated by effects such as interference from waves reflected by the boundary division of the absorbing media.

When analysing the expressions (7.93) and (7.94) it is easy to see that the first terms in the square brackets characterize the absorption and the natural radiation of direct and back waves in each layer individually, while the second terms denote the change in the absorption of waves due to their interaction (interference). This fact does not contradict the law of conservation of energy since it implies that spatial redistribution of the heat release takes place within the medium with the interaction of back waves, but the general energy balance (incident, reflected, transmitting and absorbing) is preserved, as shown for a single boundary between two absorbing media (Veremey *et al.*, 1978). Thus, in the presence of wave interference, neighbouring areas of the spectrum (even with equal parameters) may contribute different values to the resulting radiation. It is a basic fact that the value of the radiation of each layer is affected by the dielectric characteristics of the medium not only between the layer and the surface but also as a whole. Strictly speaking, it is impossible to determine the true contribution of an individual layer to the resulting radiation without knowing the full dielectric characteristics of all its surroundings.

We note that the method studied is a monochromatic approximation. It remains valid for a narrow spectral interval such that the phase difference between the harmonic components at the length of the scale of the non-uniformity is small (see section 7.6 and Popov and Sharkov, 1976).

7.7.3 Limiting cases of general theory

We would naturally expect the above general solution of the thermal radiation problem for a stratified non-uniform isothermal medium to include, in the limit, all known approximation methods for similar problems. It is not difficult to check this directly.

We assume that the medium is weakly non-uniform so that it is possible to neglect multiply-reflected waves except those at the boundary of the medium R_0. In this case, $R_j^- = 0$.

$$(|W_j|^2/\operatorname{Re} Z) = (1 - |R_0|^2)/\operatorname{Re} Z_1 \left| \prod_{m=1}^{j} \exp(\mathrm{i}k_{zm}d_m) \right|^2. \tag{7.97}$$

We denote the impedance of the layer at the boundary of the medium by Z_1. Under these conditions, equations (7.93) and (7.94) take the form

$$T_{\mathrm{br}} = \sum_{j=1}^{N} T_j(1 - |R_0|^2)(1 - \exp(-2 \operatorname{Im} k_{zj}d_j))\left|\exp(\mathrm{i}\Sigma_{m=1}^{j} k_{zm}d_m)\right|^2 \frac{\operatorname{Re} Z_j}{\operatorname{Re} Z_1}$$

$$+ T_{N+1}(1 - |R_0|^2)\left|\exp(\mathrm{i}\Sigma_{m=1}^{j} k_{zm}d_m)\right|^2 \frac{\operatorname{Re} Z_{N+1}}{\operatorname{Re} Z_1}. \tag{7.98}$$

Letting the value of d_j tend to zero and the area of the summation tend to infinity, and representing the exponent in the first factor as a series, we convert from

summation to integration

$$T_{\text{br}} = (1 - |R_0|^2) \int_0^\infty T(z)\, 2\,\text{Im}\,(k(z)\cos\theta(z)) \times \exp\left[-2\int_0^\infty \text{Im}k(z')\cos\theta(z')\,\text{d}z'\right] \frac{\text{Re}\,Z(z)}{\text{Re}\,Z(0)}\,\text{d}z. \tag{7.99}$$

The last expression agrees, within the accuracy of the notation, with the solution by WKB-method (Shulgina, 1975), which is a subcase of the general solution for the given conditions. With the additional assumptions that the variations of the dielectric constant of the medium $\text{Re}\,\varepsilon(z) \cong \text{const}$, $Z(z) \cong Z(0)$ are small and that the absorption by the medium $\text{Re}\,\dot{\varepsilon}(z) > \text{Im}\,\dot{\varepsilon}(z)$ is insignificant, and transferring to the real angle of refraction $\theta'(z) = \text{Re}\,\theta(z)$, where $k(z)\cos\theta(z) \cong k(z)/\cos\theta'(z)$, we obtain the well-known solution of the phenomenological equation of radiation transfer (ETR) (see Chapter 9)

$$T_{\text{br}} = (1 - |R|^2) \int_0^\infty T(z) \frac{2\text{Im}\,k(z)}{\cos\theta'(z)} \exp\left(-2\int_0^2 \text{Im}\,k(z')/\cos\theta'(z')\,\text{d}z'\right)\text{d}z. \tag{7.100}$$

The physical difference between (7.99) and the solution of the ERT is the calculation of the refraction-related perturbations of the outgoing thermal flux from the absorbing medium (imaginary term). Since $2\,\text{Im}\,k(z) = \gamma(z)$ is the absorption in the medium, expression (7.99) for a uniform absorbing medium may be written in the form obtained by Shulgina (1975):

$$T_{\text{br}} = \kappa(\theta, \lambda) \int_0^\infty \gamma(z) S(\theta) T(z) \exp\left(-\gamma(z') S(\theta)\,\text{d}z'\right)\text{d}z, \tag{7.101}$$

where θ is the angle of observation outside the medium measured from the nadir, and $S(\theta)$ is the refraction coefficient

$$S(\theta) = \left(\frac{\varepsilon_1 - \sin^2\theta}{\varepsilon_1(\sqrt{1 + \text{tg}^2\,\delta} - 1)}\right)^{1/2} \left[\sqrt{1 + \frac{\varepsilon_1^2 \text{tg}^2\delta}{(\varepsilon_1 - \sin^2\theta)}} - 1\right]^{1/2}. \tag{7.102}$$

Here, $\dot{\varepsilon} = \varepsilon_1(1 + \text{i}\,\text{tg}\,\delta)$ is the complex dielectric constant of the medium.

A special calculation of the refraction coefficient for a broad range of wavelengths (from 0.33 to 75 cm) and values of the angles of observation (from 0 to 89°) performed by Sharkov (1978), showed that the contribution of refraction to the polarization characteristics of the absorbing media (seawater and freshwater) is quite small: S differs from the value of this coefficient calculated for a medium with low losses by $< 4\%$, which amounts to a corresponding change in the brightness temperature of < 0.004 K.

Whence, it follows that the results of the phenomenological theory of radiative transfer hold for weakly absorbing media ($\text{tg}\,\delta \ll 1$) and are also applicable to media with strong absorption ($\text{tg}\,\delta \geq 1$, for example, seawater) provided the real part of the complex dielectric constant ($\varepsilon_1 \gg 1$) is sufficiently high; thus, the difference between the refraction coefficient and the value determined by Snell's law is small. It is for this

physical reason that methods developed for the calculation of the radio-emission of pure transparent media in due course (Troitskii, 1954, 1967; Chandrasekhar, 1960) describe the absorbing media emission adequately.

The derivation of equations (7.93)–(7.94) was based on the computation of the full losses of waves (in terms of amplitude) in the whole multi-layered structure, which is equivalent to determination of the difference in power of the incident and reflected waves and corresponds to Kirchhoff's law for stratified isothermal media, where $T_j = \text{const}$,

$$T_{\text{br}} = (1 - |R_{\Sigma}|^2)T, \tag{7.103}$$

where R_{Σ} is the reflection coefficient of water on the free-space side, taking into account all multiple reflections in the multi-layered medium. We have already used this result in section 7.5.

The comparatively simple subcase of a three-layered medium with different temperature layers was considered in due course in work by Tuchkov (1968) and Basharinov *et al.* (1968), where the direct and multiply-reflected fluxes of thermal radiation from different layers were summed to obtain the expression for the average brightness temperature (Basharinov *et al.*, 1968):

$$T_{\text{br321}} = \frac{[T_3(1 - R_{32}^2)\exp(-\tau_2) + T_2(1\exp(-\tau_2))(1 + R_{32}^2\exp(-\tau_2))](1 - R_{12}^2)}{1 - R_{12}^2 R_{32}^2\ \exp(-2\tau_2)}. \tag{7.104}$$

The value of the index 1 relates to the free space, the coefficients R_{ij} are the moduli of the Fresnel coefficients for the two media, and τ_2 is the optical depth of the intermediate layer 2.

Comparing with (7.93)–(7.94), we note that equation (7.104) involves a number of simplifications which limit its area of applicability. Firstly, it does not take account of phase relationships for multiply-reflected waves and interference effects are not considered. Instead of this, it describes their power characteristics, which is to some extent justified for a brightness temperature averaged over a sufficiently broad range of frequencies, where the term 'sufficiently' remains undetermined. For example, the sign in the denominator of (7.104) depends on the phase of the Fresnel coefficients at the two boundaries, which in turn depends on the equations for ε_2 and ε_3.

Secondly, on passing the boundaries of absorbing medium, it is not the sum of the normal components of the fluxes of wave energy which is continuous, but the normal component of the energetic flux of the field as a whole (see section 7.3). Thus, strictly speaking, the power of the passing wave t_{p12} is not equal to the difference between the incident and the reflected waves $t_{\text{p12}} \neq 1 - |R_{12}|^2$. Thirdly, as previously shown for interfering waves in an absorbing medium, there occurs a redistribution of absorption of the wave energy in space, which was described in (7.93)–(7.94) by an interference term.

For the brightness temperature of temperature of a three-layered medium with equal temperatures in the layers, (7.93)–(7.94) provides an accurate expression

$$T_{\rm br} = \frac{T_2[(1-\exp(2\beta))|1-R_{12}|^2(1+|R_{32}|^2\exp(-2\beta)) + 4\beta/\alpha\,\mathrm{Re}\,(R_{32}\exp(\mathrm{j}\psi))]\mathrm{Re}\,Z_2}{\mathrm{Re}\,Z_1|1-R_{12}R_{32}\exp(2\mathrm{i}\psi)|^2}$$
$$+ T_3|(1-R_{12})(1-R_{32})|^2\exp(-2\beta)\,\mathrm{Re}\,Z_3, \qquad (7.105)$$

where $\psi = \alpha + \mathrm{i}\beta = k_z d$, τ_2 in (7.104) corresponds to 2β, Z_j are the impedances of the media and R_{ij} are the complex (unlike (7.104)) Fresnel reflection coefficients. In this expression, it is not difficult to observe all the differences from (7.104) listed above.

7.7.4 Conditions for the method's feasibility

The method described above for analysing thermal radiation is accurate for stratified non-uniform media; in other words, it assumes strictly constant parameters of the medium and equilibrium in each layer. Let us consider in more detail the restriction of the applicability of the method to the problem of thermal radiation from real media with arbitrary parameter profiles. Firstly, at each point of space, the conditions for the applicability of the FDT should be satisfied, which implies the equilibrium of the energy distribution (in terms of degrees of freedom) and small radii of correlation τ_k of the outside fluctuating fluxes in relation to the scales of the non-uniform and non-isothermal anomalies of the medium $d_j \gg \tau_k$. Secondly, the legitimacy of the representation of the continuous parameters of the medium in the form of a stratified structure must be verified. This is not difficult, assuming relatively small errors in the computation of the characteristics of the propagation (phase and amplitude) $|\Delta\psi_j/\psi_j| \ll 1$ and the radiation $\Delta T'_{\rm br}/T'_{\rm br} \ll 1$ in each layer due to the replacement of the real parameter profiles by average values (for simplicity, the values of the parameters in the centre of the layer):

$$d_j \ll \frac{4\sqrt{6}|\varepsilon_j|}{|\partial\varepsilon_j/\partial z|}, d_j \ll 2\sqrt{\frac{6N_j}{\partial^2 T_j/\partial z^2}}. \qquad (7.106)$$

The second condition was based on the assumption that the attenuation of radiation in a layer is small. Here, d_j does not depend on the first derivative of the temperature profile.

The given estimates do not take into account wave interference within a layer, since this is impossible without using additional information about its surroundings. However, it is possible to estimate the maximum effect of interference, assuming the boundary layer is an absolute reflector. Here, condition (7.106) does not depend on the wavelength of the radiation:

$$d_j \ll \frac{|\varepsilon_j|^2}{|\partial\varepsilon_1/\partial z|}8\sqrt{\frac{3\,\mathrm{Im}\,(\sqrt{\varepsilon_j})}{|\sqrt{\varepsilon_j}|}}, d_j \ll 4\sqrt{\frac{3T_j\,\mathrm{Im}\,(\sqrt{\varepsilon_j})}{(\partial^2 T_j/\partial Z^2)|\sqrt{\varepsilon_j}|}}. \qquad (7.107)$$

For a fixed thickness of the layers, in general, the number of layers is given by $N = D/\min(d_j)$.

Naturally, the radiation of layers far from the external boundary of the medium is attenuated and the contribution of their errors to the total brightness temperature is less than that of neighbouring layers. Thus, as the distance from the boundary of the medium increases, the stringency of the conditions on the thickness of the layers decreases. Consequently, in order to decrease the overall volume of the actual calculation, it is convenient to use (other conditions remaining the same) a variable step for the subdivision of the layer, which increases with the distance from the boundary of the medium.

The previous conditions were found independently for variations of the profiles of the dielectric constants and temperature of individual layers, since joint estimation of the computational error due to their variations is very complicated. Thus, finally, the number of sublayers into which it is sufficient to divide media with complicated parameter profiles may be simply determined as a function of the convergence of numerical computations of T_{br} for a sequentially increasing number of subdivisions.

7.7.5 Spectral characteristics of thermal emission for some stratified media

The goal of this subsection is to identify the main characteristics of the field of radiation of non-isothermal, non-uniform media. These may be identified most clearly by analysis of the spectral characteristics of the thermal radiation of a series of model media, obtained by numerical modelling (relevant algorithms were described in work by Klepikov and Sharkov (1983)). Let us compare the results of applying the method described in the second section (7.7.2) with other methods, based on the example of a three-layered, non-isothermal medium (observation of a medium with $\varepsilon_1 = 1$) and the model A:

$$\varepsilon_2 = 10 + \text{i}1; \qquad T_2 = 200\,K \quad 0 < z < 10\,\text{cm}$$

$$\varepsilon_3 = 100 + \text{i}10; \quad T_3 = 300\,K \quad 10\,\text{cm} < z.$$

Figure 7.17 shows graphs of the brightness temperature against wavelength for observations in the nadir. Curves 1–5 were calculated using the accurate formulae (7.105), the WKB method (7.99), the radiation transfer equation (7.100), Kirchhoff's method (7.103) with average temperature 300 K, and formula (7.104) for an average temperature of the three-layered medium (by summing the thermal fluxes), respectively.

In the short-wave area of the frequency band, where the wavelength of the radiation is far less than the characteristic size of the non-uniformities of the medium and the radiation is largely determined by the thin surface layer, approximation methods give a good approximation to the graph of T_{br} calculated using the accurate formula. The differences in the values of T_{br} for Kirchhoff's method (curve 4) are associated with chosen value $T = 300\,\text{K}$, for which the emissivity of the medium $\kappa = 1 - |R|^2$ corresponds accurately to the value obtained by the accurate formula ($\kappa = 0.7272$).

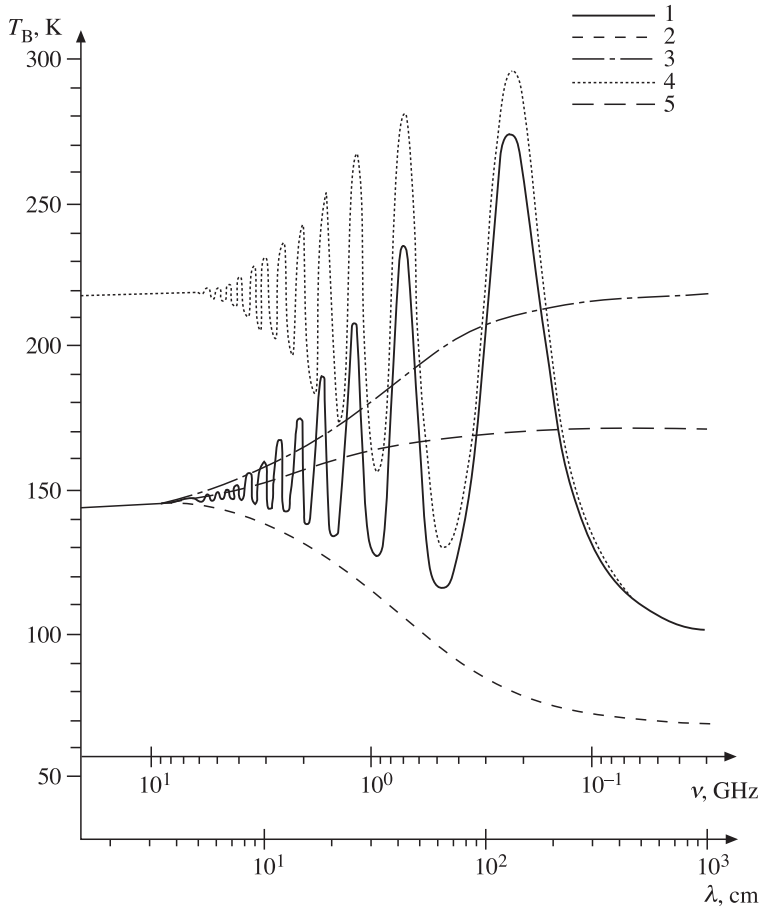

Figure 7.17. Spectral characteristics of the natural radiation of a three-layered non-isothermal medium (model A). 1–5, see explanation in text.

However, for the whole spectrum of frequencies, and particularly the long-wave area, the errors of each of the approximation methods are very significant (up to 100 K). For example, the method of summing the thermal fluxes (curve 5) gives 'clearly average' spectral variations of T_{br} without interference features. In other words, the spectral averaging built into the method is carried out over practically the full range of frequencies used. Most striking (numerical) differences are observed in the spectral variations of the curves 2 and 3 obtained by the WKB and ERT method, which are apparently very similar to each other (see formulas (7.99) and (7.100)).

Consideration of this model example shows that not one of the approximation methods provides correct calculation of the emissivity of highly non-uniform, non-isothermal media over a broad band of wavelengths.

Very large numerical differences between the spectral graphs of T_{rmbr} for the accurate method and for the approximation methods are found where relatively local temperature jumps occur in an area of interfering waves, reflected by the dielectrical non-uniformities of the medium. Figure 7.13 shows the spectral variation of the radiation ($\theta = 0$) from an isothermal three-layered medium (model B) with profiles

$$\varepsilon_2 = 1 = +\text{i}0.4, \quad 0 < z < 10\,\text{cm}$$
$$\varepsilon_3 = 100 + \text{i}10, \quad 10\,\text{cm} < z$$

calculated using Kirchhoff's law for isothermal media. The spectral variation for this medium, but with a sharp temperature anomaly $T = 900\,\text{K}$ for $7.5 < z < 7.75\,\text{cm}$ in the intermediate layer (model C), is shown in Figure 7.18. From a comparison of the two graphs it is easy to see the change in the nature of the modulation of the spectral

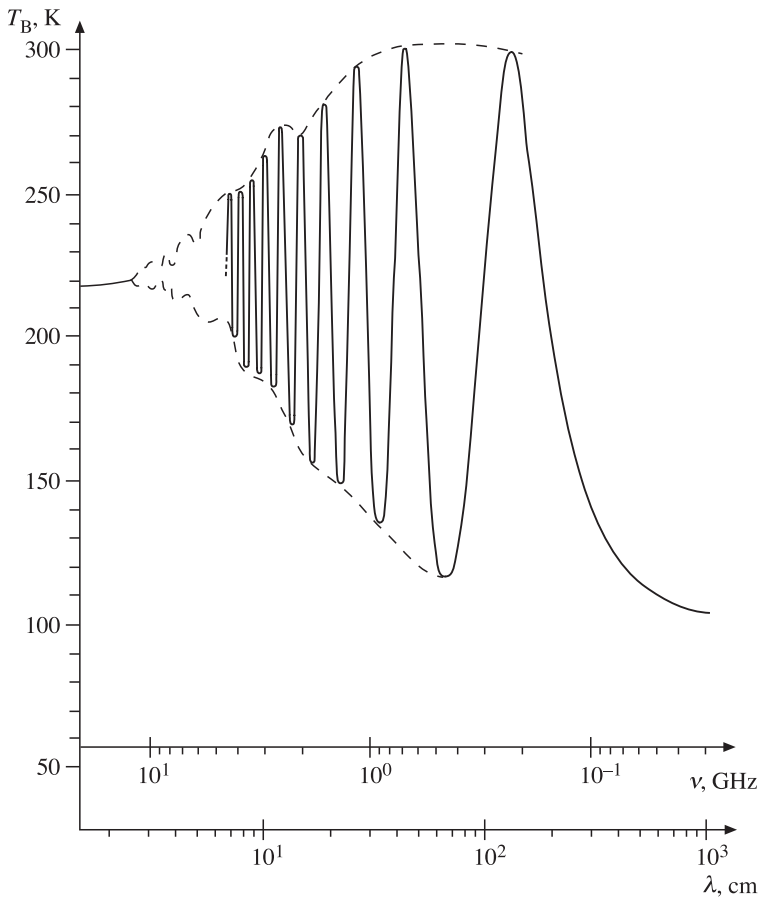

Figure 7.18. Spectral characteristics of the natural radiation of a three-layered medium (model B) with a sharp 'pulse-like' temperature anomaly.

curve of the radiation from the medium in the presence of the temperature anomaly. In fact, as a result of reflection, a mixed wave occurs in the intermediate layer; in other words, both travelling and standing waves occur. Thus, within the layer there is a special redistribution of the energy losses and consequently the different areas of the medium give different contributions to the resulting radiation. At frequencies corresponding to the position of the bulge of the standing waves at the point of a temperature jump, the contribution of the radiation of this layer to the total value T_{br} is a maximum. Conversely, when the position of the node of the standing waves and the thermal anomaly coincide, the contribution to T_{br} is a minimum. From these considerations it is clear that the maximum value of the modulation coefficient (all other conditions being equal) is attained for a temperature jump of much less than half the wavelength of the radiation. Consequently, the thinner the anomalous layer, the broader the band of frequencies in which modulation is observed. Its frequency is largely determined by the change in phase of waves from the anomalous layer to the neighbouring dielectric non-uniformity of the medium. This modulation effect is most clearly visible for a three-layered medium although it is also found in perturbed form for more complicated profiles of the dielectric parameters. A sufficient condition for modulation of the thermal radiation is the presence of a thin layer with an anomalous temperature in an area of the medium where there exist interfering waves.

Figure 7.19 and 7.20 illustrate the occurrence and relative positions of two types of modulation of the spectrum of thermal radiation from a three-layered medium, associated with the presence of a layer with anomalous values of the imaginary part of the dielectric constant and the temperature. The first effect takes the form of amplitude modulation and the second that of an additional sinusoidal component. If effects of approximately equal value are collocated, the resulting shape of the modulation will be almost one-sided (analogue of amplitude/phase modulation).

Thus, use of the accurate expressions (7.93)–(7.94) to calculate the thermal radiation from non-uniform, non-isothermal media with local anomalies and with arbitrary absorption leads to the occurrence of effects ignored by the calculations of the approximation methods (WKB method, theory of radiative transfer, Kirchhoff's law etc.).

It is certainly interesting to analyse the errors in the calculations of the spectral variations of the radiation from media with smoothly varying parameters as a function of the number of subdivisions N of the layer. Figures 7.21(a) and (b) show the results of numerical calculations of T_{br} for two typical profiles of the complex dielectric coefficients and the temperature, namely a linear and an exponential profile. In the calculations, we chose two ways of dividing the non-uniform area of the medium of thickness D into layers: a linear method, in which the thickness of all the layers was the same $d_j = D/N$, and an exponential method in which the thickness of the layers increased as the distance from the boundary of the medium

$$d_j = 2d_{j-1}, \sum_{j=1}^{N} d_j = D.$$

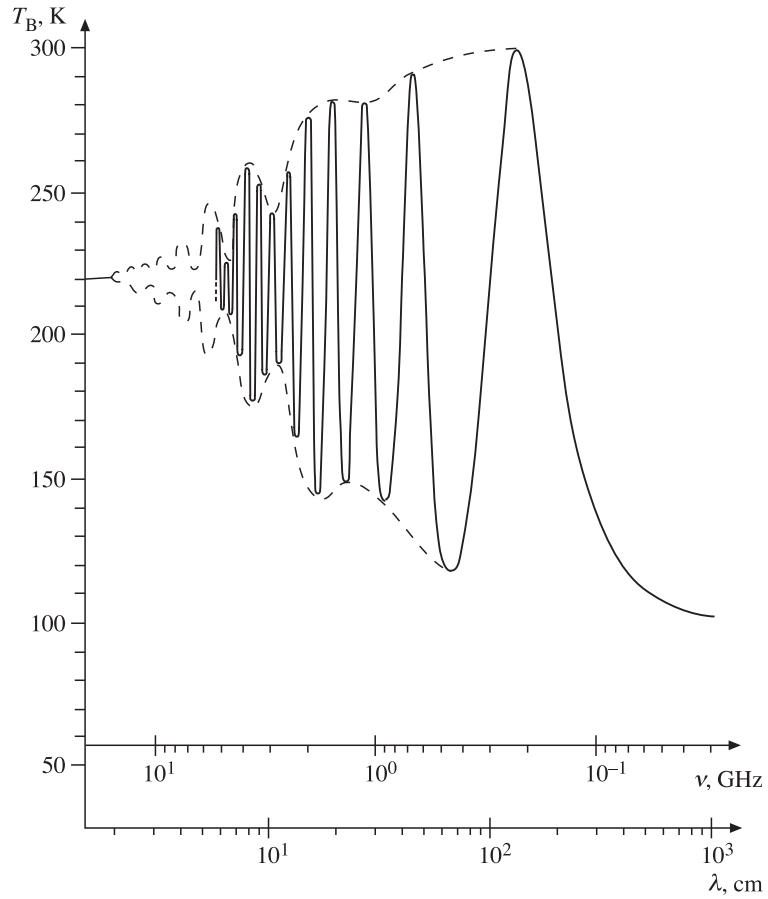

Figure 7.19. Spectral characteristics of the natural radiation of a three-layered medium with a 'pulse-like' anomaly of dielectric losses (model C).

From the figure, it is easy to see that in the band of wavelengths from ~0.1 to 100 cm there are considerable variations in the radiation spectra. For $N = 128$, for both types of profiles of the parameters, the radiation spectra exhibit a stationary form, and are practically unchanged for small variations of the number of subdivisions. Thus, they may be assumed to be 'true' (in the asymptotic sense) and compared with radiation spectra for other values of N. Maximum errors in the spectra as a function of N are given in Table 7.1.

It is clear from the table that the exponential subdivision into layers provides for faster and more uniform convergence of the results throughout the whole spectral interval, this being more noticeable for the exponential profiles of the parameters.

In this way, based on the application of a generalization of Kirchhoff's law to a model of a stratified medium with a planar boundary, we have obtained a closed-form for thermal radiation in a monochromatic approximation, taking into account

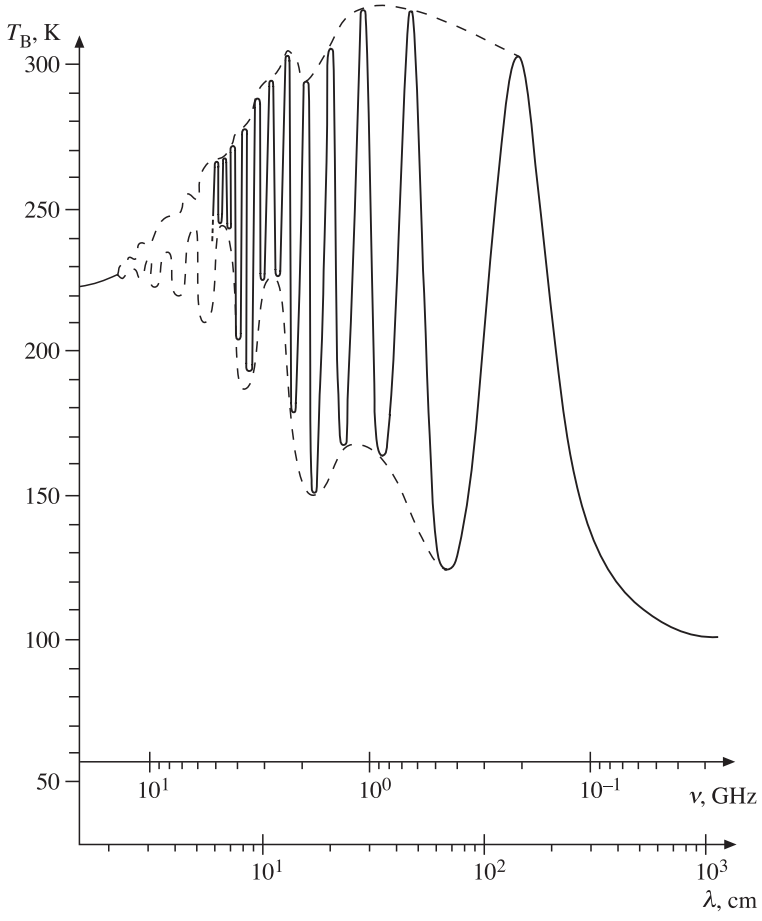

Figure 7.20. Spectral characteristics of the natural radiation of a three-layered medium with an anomalous value of the dielectric losses (model C) and with a sharp 'pulse-like' temperature anomaly.

Table 7.1. Maximum errors in T_{br}, K

Number of layers	Parameter profile			
	Linear		Exponential	
	Type of subdivision			
	Linear	Exponential	Linear	Exponential
1	22	–	17	–
4	12	8	15	7
16	2	2	6	1

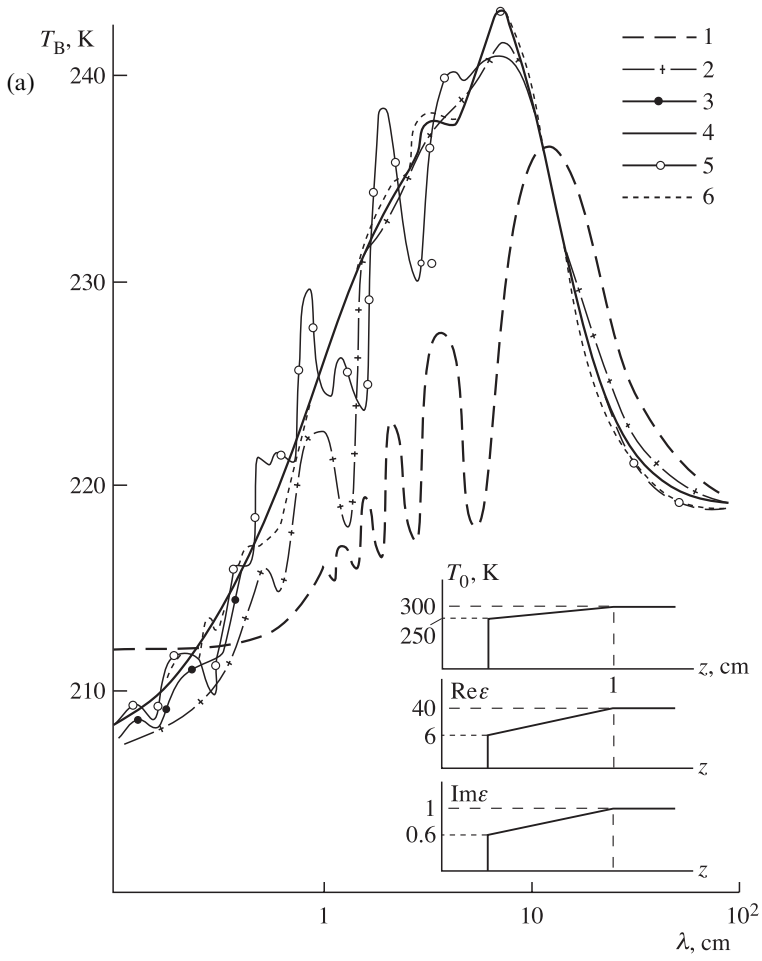

Figure 7.21. Spectral characteristics of natural radiation as a function of the number of subdivisions, N, of the layer in the medium, with linear (a) and exponential (b) stratifications of the dielectric and thermal parameters: 1, a single layer; 2, 4 layers; 3, 16; 4, 128 (linear subdivision); 5, 4; 6, 16 (exponential subdivision).

interference effects. The solution involves a dependence on the wavelength, the angle of observation and the type of polarization of the radiation. It is shown that, for specific conditions satisfied for most types of real media in the microwave and IR band, this solution enables us to determine the spectral characteristics of the thermal radiation from a vertically non-uniform, non-isothermal medium with arbitrary absorption, with reasonable accuracy. The solution also includes known methods of calculating the brightness temperature such as solution of the radiation transfer equation, Kirchhoff's law for isothermal media and solution by the WKB method, and is a generalization of these.

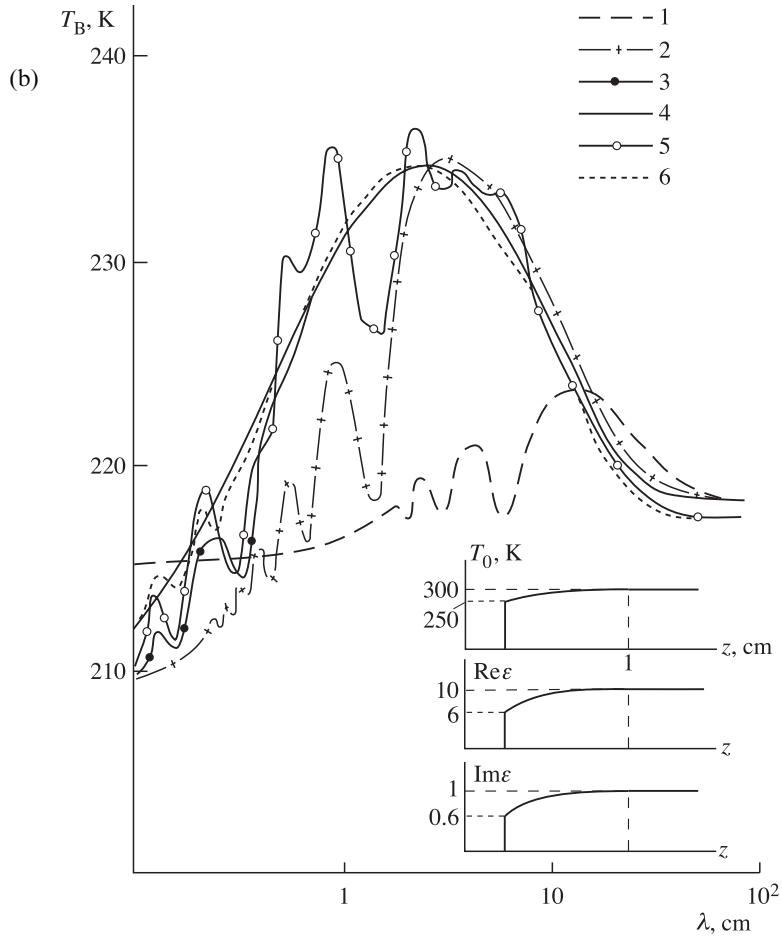

Figure 7.21 (b)

Using the method described we have developed a computer-based algorithm and carried out numerical analysis of the thermal radiation spectra for a number of characteristic cases of non-uniform, non-isothermal media. The greatest differences between the spectral variations of the radiation for this method and those for existing methods occur in the presence of relatively local temperature jumps of width less than the wavelength. Here, in addition to the usual modulation of the spectral characteristics of the radiation due to interfering waves reflected by the dielectric non-uniformities of the medium, there is additional modulation in the form of sinusoidal components which are damped as the wavelength of the radiation decreases.

The method described in this section and the computational algorithm may be used to solve more complicated problems of thermal radiation, for example, for media with three-layered temperature and dielectric anomalies with rough boundary divisions, and also for media with random parameter non-uniformities.